

# Similarity Search for Efficient Active Learning and Search of Rare Concepts

Cody Coleman<sup>1\*</sup>, Edward Chou<sup>2</sup>, Sean Culatana<sup>2</sup>, Peter Bailis<sup>1</sup>,  
Alexander C. Berg<sup>3</sup>, Roshan Sumbaly<sup>2</sup>, Matei Zaharia<sup>1</sup>, I. Zeki Yalniz<sup>2</sup>

<sup>1</sup>Stanford University, <sup>2</sup>Facebook AI, <sup>3</sup>Facebook AI Research

## Abstract

Many active learning and search approaches are intractable for industrial settings with billions of unlabeled examples. Existing approaches, such as uncertainty sampling or information density, search globally for the optimal examples to label, scaling linearly or even quadratically with the unlabeled data. However, in practice, data is often heavily skewed; only a small fraction of collected data will be relevant for a given learning task. For example, when identifying rare classes, detecting malicious content, or debugging model performance, the ratio of positive to negative examples can be 1 to 1,000 or more. In this work, we exploit this skew in large training datasets to reduce the number of unlabeled examples considered in each selection round by only looking at the nearest neighbors to the labeled examples. Empirically, we observe that learned representations effectively cluster unseen concepts, making active learning very effective and substantially reducing the number of viable unlabeled examples. We evaluate several active learning and search techniques in this setting on three large-scale datasets: ImageNet, Goodreads spoiler detection, and OpenImages. For rare classes, active learning methods need as little as 0.31% of the labeled data to match the average precision of full supervision. By limiting active learning methods to only consider the immediate neighbors of the labeled data as candidates for labeling, we need only process as little as 1% of the unlabeled data while achieving similar reductions in labeling costs as the traditional global approach. This process of expanding the candidate pool with the nearest neighbors of the labeled set can be done efficiently and reduces the computational complexity of selection by orders of magnitude.

## 1 Introduction

Large-scale unlabeled datasets contain millions or billions of examples spread over a wide variety of underlying concepts [7, 38, 36, 32, 25, 19, 31, 1, 5, 20]. Often, these massive datasets skew towards a relatively small number of common concepts, such as cats, dogs, and people. Rare concepts, such as harbor seals, may only appear in a handful of examples. However, in many settings, performance on these rare concepts is critical [3, 32, 16, 11, 17]. For example, harmful or malicious content may comprise a small percentage of user-generated content, but it can have an outsize impact on the overall user experience [32]. Similarly, when debugging model behavior for safety-critical applications like autonomous vehicles or dealing with representational biases in models, obtaining data that captures rare concepts allows modelers to combat blind spots in model performance [16, 11, 3, 17]. Even a simple prediction task like stop sign detection can be challenging given the diversity of real-world data. Stop signs may appear in a variety of conditions (e.g., on a wall or held by a person), be heavily occluded, or have modifiers (e.g., “Except Right Turns”) [17]. While large-scale datasets are core to addressing these issues, finding the relevant examples for these long-tail tasks is challenging.

\*Correspondence: cody@cs.stanford.edu

Active learning has the potential to automate the process of identifying these rare, high value data points significantly, but existing methods become intractable at this scale. Specifically, the goal of active learning is to reduce the cost of labeling [29]. To this end, the learning algorithm is allowed to choose which data to label based on uncertainty (e.g., the entropy of predicted class probabilities) or other heuristics [28, 29, 21]. Because of a concentrated focus on labeling costs, existing techniques, such as uncertainty sampling [21] or information density [30], perform multiple selection rounds and iterate over the entire unlabeled data to identify the optimal example or batch of examples to label and scale linearly or even quadratically with the size of the unlabeled data. However, computational efficiency is becoming an impediment as the size of datasets and model complexities have increased [2]. Recent work has tried to address this problem with sophisticated methods to select larger and more diverse batches of examples in each selection round and reduce the total number of rounds needed to reach the target labeling budget [26, 18, 8, 23, 13]. Nevertheless, these approaches still scan over all of the examples to find the optimal examples to label in each selection round and can be intractable for large-scale unlabeled datasets. For example, running a single inference pass over 10 billion images with a ResNet-50 model [10] would take 38 exaFLOPs.

In this work, we propose Similarity search for Efficient Active Learning and Search (SEALS) to restrict the candidates considered in each selection round and vastly reduce the computational complexity of active learning and search methods. Empirically, we find that learned representations from pre-trained models effectively cluster many unseen and rare concepts. We exploit this latent structure to improve the computational efficiency of active learning and search methods by only considering the nearest neighbors of the currently labeled examples in each selection round. Leveraging advances in similarity search and highly optimized implementations, finding the nearest neighbors for each labeled example can be done in logarithmic time or even in constant time with approximate approaches [4, 15]. While constructing the index for similarity search requires at least a linear pass over the unlabeled data, this computational cost is effectively amortized over many selection rounds or other applications. As a result, our SEALS approach enables selection to scale with the size of the labeled data rather than the size of the unlabeled data, making active learning and search tractable on datasets with billions of unlabeled examples.

We empirically evaluate SEALS for both active learning and search on three large scale datasets: ImageNet [25], Goodreads spoiler detection [32], and OpenImages [19]. Each dataset has millions to tens of millions of examples. We selected 604 concepts spread across these datasets that range in prevalence from 3.2% to 0.002% (1 in 50,000) of the training examples. We evaluated three selection strategies for each concept: max entropy uncertainty sampling [21], information density [30], and most-likely positive [34, 33, 13]. Across datasets, selection strategies, and the vast majority of concepts, SEALS achieved similar model quality and nearly the same recall of the positive examples as the baseline approaches, while improving the computational complexity by orders of magnitude. On ImageNet with a budget of 2,000 binary labels per concept ( $\sim 0.31\%$  of the unlabeled data), all baseline and SEALS approaches were within 0.011 mAP of full supervision and recalled over 50% of the positive examples. For each selection strategy, the SEALS approach was within 0.001 mAP of the baseline equivalent. For information density, which scales quadratically, that trade-off reduced the time for a selection round from over 95 minutes to 1.4 seconds, over a  $4000\times$  improvement. On OpenImages, SEALS reduced the candidate pool to 1% of the unlabeled data on average while remaining within 0.013 mAP and 0.1% recall of the baseline approaches. On Goodreads, SEALS model quality and recall were indistinguishable from the baseline approaches, but only considered less than 1% of the unlabeled data in the candidate pool. For both Goodreads and OpenImages, information density over all the data did not complete a single round after days of computation, while SEALS reduced the runtime to seconds. Together, these results demonstrate that SEALS dramatically improves the computational efficiency of these selection strategies while maintaining selection quality, making active learning and search of rare concepts tractable for large scale data.

## 2 Related work

**Active learning**'s iterative retraining combined with the high computational complexity of deep learning models has led to significant work on computational efficiency [26, 18, 23, 8, 35, 22, 37]. One branch of recent work has focused on selecting large batches of data to minimize the amount of retraining and reduce the number of selection rounds necessary to reach a target budget [26, 18, 23]. These approaches introduce novel techniques to avoid selecting highly similar or redundant examples

and ensure the batches are both informative and diverse. In comparison, our work aims to reduce the number of examples considered in each selection round and complements existing work on batch active learning. Many of these approaches sacrifice computational complexity to ensure diversity, and their selection methods can scale quadratically with the size of the unlabeled data. Combined with our method, these selection methods scale with the size of the labeled data rather than the unlabeled data. Outside of batch active learning, other work has tried to improve computational efficiency by either using much smaller models as cheap proxies during selection [35, 8] or by generating examples [22, 37]. Using a smaller model reduces the amount of computation per example, but unlike our approach, it still requires making multiple passes over the entire unlabeled pool of examples. The generative approaches [22, 37], however, enable sub-linear run-time complexity like our approach. Unfortunately, they struggle to match the label-efficiency of traditional approaches because the quality of the generated examples is highly variable.

**Active Search** is a sub-area of active learning that focuses on highly skewed class distributions [9, 12–14]. Rather than optimizing for model quality, active search aims to find as many examples from the minority class as possible. Prior work has focused on applications such as drug discovery, where the dataset sizes are limited, and labeling costs are exceptionally high. Our work similarly focuses on skewed distributions. However, we consider novel active search settings in image and text where the available unlabeled datasets are much larger, and computational efficiency is a significant bottleneck.

### 3 Methods

In this section, we outline the problems of active learning (Section 3.1) and search (Section 3.2) formally as well as the selection methods we accelerate using SEALS. For both, we examine the pool-based batch setting, where all of the unlabeled data is available at once, and examples are selected in batches to improve computational efficiency, as mentioned above. Then in Section 3.3, we describe our SEALS approach and how it further improves computational efficiency in both settings.

#### 3.1 Active learning

Pool-based active learning is an iterative process that begins with a large pool of unlabeled data  $U = \{\mathbf{x}_1, \dots, \mathbf{x}_n\}$ . Each example is sampled from the space  $\mathcal{X}$  with an unknown label from the label space  $\mathcal{Y} = \{1, \dots, C\}$  as  $(\mathbf{x}_i, y_i)$ . We additionally assume a feature extraction function  $G_z$  to embed each  $\mathbf{x}_i$  as a latent variable  $G_z(\mathbf{x}_i) = \mathbf{z}_i$  and that the  $C$  concepts are unequally distributed. Specifically, there are one or more valuable rare concepts  $R \subset C$  such that  $\frac{n}{C} \gg \sum_{i=1}^n \mathbb{1}\{y_i = r\}$  for  $r \in R$ . For simplicity, we frame this as  $|R|$  binary classification problems solved independently rather than 1 multi-class classification problem with  $|R|$  concepts. Initially, each rare concept has a small number of positive examples and several negative examples that serve as a labeled seed set  $L_r^0$ . The goal of active learning is to take this seed set and select up to a budget of  $T$  examples to label that produces a model  $A_r^T$  that achieves low error. For each round  $t$  in pool-based active learning, the most informative examples are selected according to the selection strategy  $\phi$  from a pool of candidate examples  $\mathcal{P}_r$  in batches of size  $b$  and labeled, as shown in Algorithm 1.

---

#### Algorithm 1 BASELINE APPROACH

---

**Input:** unlabeled data  $U$ , labeled seed set  $L_r^0$ ,  
feature extractor  $G_z$ , selection strategy  $\phi(\cdot)$ ,  
batch size  $b$ , labeling budget  $T$

```

1:  $\mathcal{L}_r = \{(G_z(\mathbf{x}), y) \mid (\mathbf{x}, y) \in L_r^0\}$ 
2:  $\mathcal{P}_r = \{G_z(\mathbf{x}) \mid \mathbf{x} \in U \text{ and } (\mathbf{x}, \cdot) \notin L_r^0\}$ 
3: repeat
4:    $A_r = \text{train}(\mathcal{L}_r)$ 
5:   for 1 to  $b$  do
6:      $\mathbf{z}^* = \arg \max_{\mathbf{z} \in \mathcal{P}_r} \phi(\mathbf{z})$ 
7:      $\mathcal{L}_r = \mathcal{L}_r \cup \{(\mathbf{z}^*, \text{label}(\mathbf{x}^*))\}$ 
8:      $\mathcal{P}_r = \mathcal{P}_r - \mathbf{z}^*$ 
9:   end for
10: until  $|\mathcal{L}_r| = T$ 
```

---



---

#### Algorithm 2 SEALS APPROACH

---

**Input:** unlabeled data  $U$ , labeled seed set  $L_r^0$ ,  
feature extractor  $G_z$ , selection strategy  $\phi(\cdot)$ ,  
batch size  $b$ , labeling budget  $T$ ,  $k$ -nearest  
neighbors implementation  $\mathcal{N}(\cdot, \cdot)$

```

1:  $\mathcal{L}_r = \{(G_z(\mathbf{x}), y) \mid (\mathbf{x}, y) \in L_r^0\}$ 
2:  $\mathcal{P}_r = \cup_{(\mathbf{z}, y) \in \mathcal{L}_r} \mathcal{N}(\mathbf{z}, k)$ 
3: repeat
4:    $A_r = \text{train}(\mathcal{L}_r)$ 
5:   for 1 to  $b$  do
6:      $\mathbf{z}^* = \arg \max_{\mathbf{z} \in \mathcal{P}_r} \phi(\mathbf{z})$ 
7:      $\mathcal{L}_r = \mathcal{L}_r \cup \{(\mathbf{z}^*, \text{label}(\mathbf{x}^*))\}$ 
8:      $\mathcal{P}_r = \mathcal{P}_r \cup \mathcal{N}(\mathbf{z}^*, k) - \mathbf{z}^*$ 
9:   end for
10: until  $|\mathcal{L}_r| = T$ 
```

---

Table 1: Computational complexity for each selection strategy.

Selection Strategy $\phi$	Baseline Complexity ( $ \mathcal{P}_r  =  U $ )	SEALS Complexity ( $ \mathcal{P}_r  \leq k L_r $ )
MaxEnt [21]	$O( U )$	$O(k L_r )$
ID [30]	$O( U ^2)$	$O(k^2 L_r ^2)$
MLP [34, 33, 13]	$O( U )$	$O(k L_r )$

For the baseline approach,  $\mathcal{P}_r = \{G_z(\mathbf{x}) \mid \mathbf{x} \in U\}$ , meaning that all the unlabeled examples are considered to find the global optimal according to  $\phi$ . Between each round, the model  $A_r^t$  is trained on all of the labeled data  $L_r^t$ , allowing the selection process to adapt.

In this paper, we consider two selection strategies, **max entropy (MaxEnt)** uncertainty sampling [21]:

$$\phi_{\text{MaxEnt}}(\mathbf{z}) = - \sum_{\hat{y}} P(\hat{y}|\mathbf{z}; A_r) \log P(\hat{y}|\mathbf{z}; A_r)$$

and **information density (ID)** [30]:

$$\phi_{\text{ID}}(\mathbf{z}) = \phi_{\text{MaxEnt}}(\mathbf{z}) \times \left( \frac{1}{|\mathcal{P}_r|} \sum_{\mathbf{z}_p \in \mathcal{P}_r} \text{sim}(\mathbf{z}, \mathbf{z}_p) \right)^\beta$$

where  $\text{sim}(\mathbf{z}, \mathbf{z}_p)$  is the cosine similarity of the embedded examples and  $\beta = 1$ . While max entropy uncertainty sampling only requires a linear pass over the unlabeled data, ID scales quadratically, as shown in Table 1, because it weights the informativeness of each example by its similarity to all other examples. Also, note that for binary classification, max entropy uncertainty sampling is equivalent to least confidence and margin sampling, which are also popular criteria for uncertainty sampling [27].

We explored the greedy k-centers approach from Sener and Savarese [26] but found that it never outperformed random sampling for our experimental setup. Unlike MaxEnt and ID, greedy k-centers does not consider the predicted labels. It tries to achieve high coverage over the entire candidate pool, of which rare concepts make up a small fraction by definition, making it ineffective for our setting.

### 3.2 Active search

Active search is closely related to active learning, so much of the formalism from Section 3.1 carries over. The critical difference is that rather than selecting examples to label that minimize error, the goal of active search is to maximize the number of examples from the target concept  $r$ , expressed with the natural utility function  $u(L_r) = \sum_{(\mathbf{x}, y) \in L_r} \mathbb{1}\{y = r\}$ . As a result, different selection strategies are favored, but the overall algorithm is the same as Algorithm 1.

In this paper, we consider an additional selection strategy to target the active search setting, **most-likely positive (MLP)** [34, 33, 13]:

$$\phi_{\text{MLP}}(\mathbf{z}) = P(r|\mathbf{z}; A_r)$$

Because active learning and search are similar, we evaluate all the selection criteria from Sections 3.1 and 3.2 in terms of both the error the model achieves and the number of positive examples.

### 3.3 Similarity search for efficient active learning and search (SEALS)

In this work, we propose SEALS to accelerate the inner loop of active learning and search by restricting the candidate pool of unlabeled examples. To apply SEALS, we use an efficient method for similarity search of the embedded examples [6, 15] and make two modifications to the baseline approach, as shown in Algorithm 2:

1. The candidate pool  $\mathcal{P}_r$  is restricted to the nearest neighbors of the labeled examples.
2. After every example is selected, we find its  $k$  nearest neighbors and update  $\mathcal{P}_r$ .

Restricting the candidate pool  $\mathcal{P}_r$  to the  $k$ -nearest neighbors of the labeled examples means we only apply the selection strategy to at most  $k|L_r|$  examples. This can be done transparently for many selection strategies making it applicable to a wide range of active learning and search methods, even beyond the ones considered here. Finding the  $k$ -nearest neighbors for each newly labeled example adds overhead, but this can be calculated exactly in logarithmic time [4] or approximately in constant time [6, 15] relative to the size of the unlabeled data. As a result, the computational complexity of each selection round scales with the size of the labeled dataset rather than the unlabeled dataset, as shown in Table 1. While constructing the index for similarity search requires at least a linear pass over the unlabeled data, this computational cost is effectively amortized over many selection rounds, concepts, or other applications. In practice, similarity search is a critical workload behind many applications, including recommendation. While the search index can be heavily optimized and tuned for the specific data distribution, we use locality-sensitive hashing (LSH) [6] implemented in Faiss [15] for simplicity and accessibility. LSH is data agnostic and applies a series of lightweight hash functions that only require one pass over the data, meaning the cost amortizes quickly.

## 4 Results

We applied SEALS to three selection strategies and performed active learning and search on three datasets: ImageNet [25], OpenImages [19], and Goodreads [32]. Section 4.1 details the experimental setup for each dataset and specifies the inputs used for both the baseline approach (Algorithm 1) and our proposed method, SEALS (Algorithm 2). Section 4.2 and Section 4.3 present the empirical results for active learning and active search, respectively.

Across selection strategies, datasets, and concepts, SEALS performs similarly to the baseline approaches while only considering a fraction of the unlabeled data  $U$  in the candidate pool for each concept  $\mathcal{P}_r$ . For  $\phi_{\text{MaxEnt}}$  and  $\phi_{\text{MLP}}$ , the computational savings were directly proportional to  $\frac{|U|}{k|L_r|}$ . For  $\phi_{\text{ID}}$ , the computational complexity scaled quadratically with the  $|\mathcal{P}_r|$ , making the baseline approach intractable on the larger datasets. However, with SEALS applied,  $\phi_{\text{ID}}$  worked for all three datasets, representing a runtime improvement of orders of magnitude. Finally, Section 4.4 explores the latent structure of the selected concepts through the derived nearest neighbor graphs and embeddings. For ImageNet and OpenImages, unseen concepts were tightly clustered in a small number of connected components. For Goodreads, the majority of examples fell into a single connected component for moderate values of  $k$  but were spread almost uniformly in the latent space. Generally,  $k$  allowed SEALS to smoothly trade-off between label and computational efficiency.

### 4.1 Experimental setup

Across all datasets and selection strategies, we followed the same general procedure for both active learning and search. Because we are interested in rare concepts, we kept the number of initial positive examples small. We evaluated three settings, with 5, 20, and 50 positives, but only included the results with the smallest size in this section. The others are shown in the supplementary material. For each setting, negative examples were randomly selected at a ratio of 19 negative examples to every positive example to form the seed set  $L_r^0$ . The slightly higher number of negatives in the initial seed set improved average precision on the validation set across all three datasets. The batch size  $b$  for each selection round was the same as the size of the initial seed set. For the seed set of 5 positive and 95 negative examples shown below,  $b$  was 100, and the labeling budget  $T$  was 2,000 examples.

As the binary classifier for each concept  $A_r$ , we used logistic regression trained on the embedded examples. For active learning, we calculated average precision on the test data for each binary concept classifier after each selection round. For active search, we count the number of positive examples labeled so far. We take the mean average precision (mAP) and number of positives across concepts, run each experiment 5 times, and report the mean and standard deviation.

We split the data, selected concepts, and created embeddings as detailed below and summarized in Table 2. Note that our approach does not constrain the choice of  $G_z$ , which allows for many network architectures. As representations continue to improve with new self-supervision, generative, or transfer learning techniques, SEALS is still applicable and performance will also likely improve.

**ImageNet** [25] has 1.28 million training images spread almost equally over 1000-classes. To simulate rare concepts, we split the data in half, using 500 classes to train the feature extractor  $G_z$  and treating

Table 2: Summary of datasets

	Number of Concepts ( $ R $ )	Embedding Model ( $G_z$ )	Number of Examples ( $ U $ )	Fraction Positive ( $\frac{\sum \mathbb{1}\{y=r\}}{ U }$ )
ImageNet [25]	450	ResNet-50 [10] (500 classes)	639,906	0.114-0.203%
OpenImages [19]	153	ResNet-50 [10] (1000 classes)	6,816,296	0.002-0.088%
Goodreads spoiler detection [32]	1	Sentence-BERT [24]	14,128,124	3.224%

the other 500 classes as unseen concepts. For  $G_z$ , we used ResNet-50 [10] but added a bottleneck layer before the final output to reduce the dimension of the embeddings to 256. We kept all of the other training hyperparameters the same as in He et al. [10]. We extracted features from the bottleneck layer and applied  $l^2$  normalization. In total, the 500 unseen concepts had 639,906 training examples that served as the unlabeled pool. We used 50 concepts for validation, leaving the remaining 450 concepts for our final experiments. The number of examples for each concept varied slightly, ranging from 0.114-0.203% of the unlabeled pool. The 50,000 validation images were treated as the test set.

**OpenImages** [19] has 7.34 million images with human-verified labels spread over 19,958 classes, taken as an unbiased sample from Flickr. However, only 6.82 million images were still available in the training set at the time of writing. As a feature extractor, we took ResNet-50 pre-trained on all of ImageNet and used the  $l^2$  normalized output from the bottleneck layer as our feature extractor. As rare concepts, we randomly selected 200 classes with between 100 to 6,817 positive training examples. We reviewed the selected classes and removed 47 classes that overlapped with ImageNet. The remaining 153 classes appeared in 0.002-0.088% of the unlabeled data. We used the same hyperparameters as the ImageNet experiments and the OpenImages predefined test split for evaluation.

**Goodreads spoiler detection** [32] has 17.67 million sentences with binary spoiler annotations. For  $G_z$ , we used a pre-trained Sentence-BERT model (SBERT-NLI-base) [24], applied PCA whitening to reduce the dimension to 256, and performed  $l^2$  normalization. Following Wan et al. [32], we used 3.53 million sentences for testing (20%), 10,000 sentences as the validation set, and the remaining 14.13 million sentences as the unlabeled pool. Spoilers made up 3.224% of the unlabeled pool.

## 4.2 Active learning

Across datasets and selection strategies, SEALS performed similarly to the baseline approaches that considered all of the unlabeled data in the candidate pool, as shown in Figure 1.

**ImageNet.** With a labeling budget of 2,000 examples per concept ( $\sim 0.31\%$  of  $|U|$ ), all baseline and SEALS approaches ( $k = 100$ ) were within 0.011 mAP of the 0.699 mAP achieved with full supervision. In contrast, random sampling (Random-All) only achieved 0.436 mAP. MLP-All, MaxEnt-All, and ID-All achieved mAPs of 0.693, 0.695, and 0.688, respectively, while the SEALS equivalents were all within 0.001 mAP at 0.692, 0.695, and 0.688 respectively. The reduced skew from the nearest neighbor expansion of the initial seed set only accounted for a small part of the improvement, as demonstrated by Random-SEALS, which achieved an mAP of 0.498.

**OpenImages.** The gap between the baseline approaches and SEALS widened slightly for Open-Images. At 2,000 labels per concept ( $\sim 0.029\%$  of  $|U|$ ), MaxEnt-All and MLP-All achieved 0.399 and 0.398 mAP, respectively, while MaxEnt-SEALS and MLP-SEALS both achieved 0.386 mAP. Increasing  $k$  to 1,000 significantly narrowed this gap for MaxEnt-SEALS and MLP-SEALS, improving mAP to 0.395, as shown in the supplementary material (Figure 7). Moreover, SEALS made information density tractable on OpenImages by reducing the candidate pool to 1% of the unlabeled data, whereas ID-All ran for four days in wall-clock time without completing a single selection round.

**Goodreads.** At a labeling budget of 2,000 examples, all the selection strategies were indistinguishable from random sampling. Increasing the labeling budget did not help, as shown in the supplementary material (Figure 5). Unlike ImageNet and OpenImages, Goodreads had a much higher fraction of positive examples (3.224%), and the examples were not tightly clustered as described in Section 4.4.

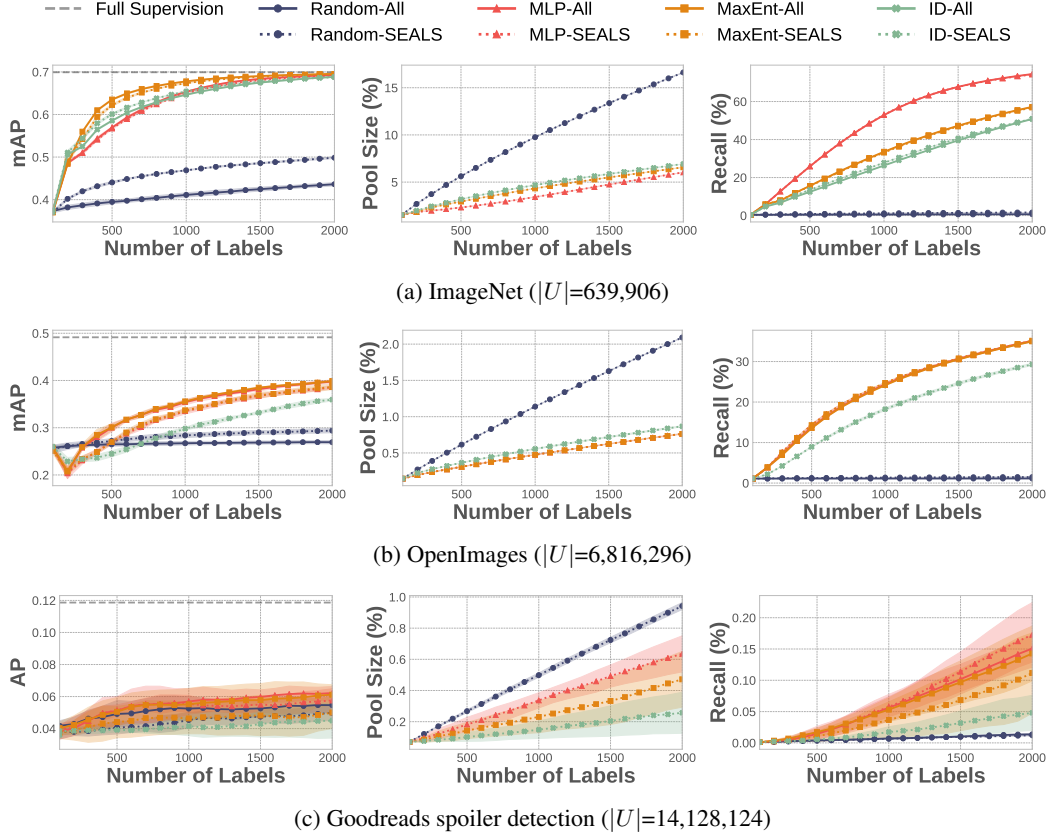


Figure 1: Active learning and search on ImageNet (top), OpenImages (center), and Goodreads (bottom). Across datasets and strategies, SEALS with  $k = 100$  performs similarly to the baseline approach in terms of both the error the model achieves for active learning (left) and the recall of positive examples for active search (right), while only considering a fraction of the data  $U$  (middle).

### 4.3 Active search

As shown in Figure 1, our SEALS approach recalled nearly the same number of positive examples as the baseline approaches did for all of the considered concepts, datasets, and selection strategies.

**ImageNet.** Unsurprisingly, MLP-All and MLP-SEALS significantly outperformed all of the other selection strategies for active search. At 2,000 labeled examples per concept, both approaches recalled over 74% of the positive examples for each concept at 74.5% and 74.2% recall, respectively. MaxEnt-All and MaxEnt-SEALS had a similar gap of 0.4%, labeling 57.2% and 56.8% of positive examples, while ID-All and ID-SEALS were even closer with a gap of only 0.1% (50.8% vs. 50.9%). Nearly all of the gains in recall are due to the selection strategies rather than the reduced skew in the initial seed set, as Random-SEALS only increased the recall by less than 1.0% over Random-All.

**OpenImages.** The gap between the baseline approaches and SEALS was even closer on OpenImages despite considering a much smaller fraction of the overall unlabeled pool. MLP-All, MLP-SEALS, MaxEnt-SEALS, and MaxEnt-All were all within 0.1% with  $\sim 35\%$  recall at 2,000 labels per concept. ID-SEALS had a lower recall of 29.3% but scaled nearly as well as the linear approaches.

**Goodreads.** All of the active selection strategies outperformed random sampling by up to an order of magnitude. There was not a clear separation between MaxEnt and MLP or SEALS and the baseline approaches. MLP-ALL and MLP-SEALS recalled  $0.15 \pm 0.02\%$  and  $0.17 \pm 0.05\%$ , respectively, while MaxEnt-All and MaxEnt-SEALS achieved  $0.14 \pm 0.04\%$  and  $0.11 \pm 0.06\%$  recall respectively. Increasing the labeling budget to 50,000 examples, increased recall to  $\sim 3.7\%$  for MaxEnt and MLP, as shown in Figure 5 of the supplementary material. ID-SEALS performed better than random sampling but worse than the other strategies.

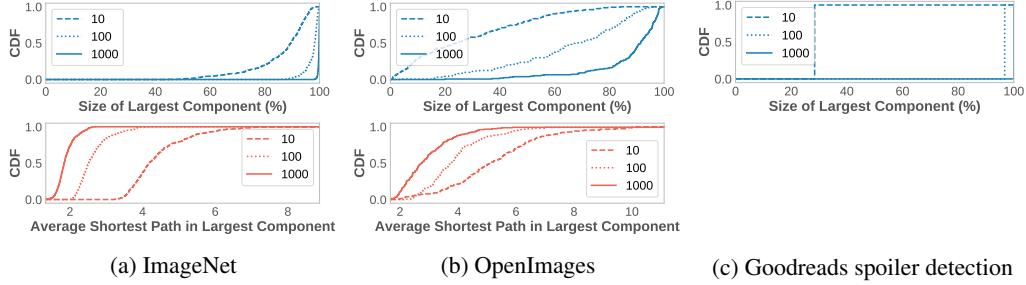


Figure 2: Measurements of the latent structure of unseen concepts in ImageNet (left), OpenImages (middle), and Goodreads spoiler detection (right). Across datasets, the  $k$ -nearest neighbor graph of unseen concepts is well connected, forming large connected components (top) for even moderate values of  $k$ . The components are tightly packed, leading to short paths between examples (bottom).

#### 4.4 Latent structure of unseen concepts

To better understand why and when SEALS works, we analyzed the nearest neighbor graph across concepts and values of  $k$ . Figure 2 shows the cumulative distribution functions (CDF) for the largest connected component within each concept and the average length of the shortest paths between examples in that component. The largest connected component of the nearest-neighbor graph gives a sense of how much of the concept SEALS can reach, while the average shortest path serves as a proxy for how long it will take to explore the space.

**ImageNet.** The unseen concepts in ImageNet had the best latent structure out of all three datasets. For most concepts, the largest connected component contained the majority of examples, and the paths between examples were very short. These tight clusters help to explain why so few examples are needed to learn accurate binary concept classifiers, as shown in Section 4.2, and why  $\sim 74\%$  of positive examples on average can be recovered while only labeling  $\sim 0.31\%$  of the entire pool.

**OpenImages.** Rare concepts were more fragmented, but each component was fairly tight, leading to short paths between examples. This fragmentation partly explains the gap between SEALS and the baseline approaches in Section 4.2, and why increasing  $k$  helped to close it.

**Goodreads.** The large number of positive examples in the Goodreads dataset limited the analysis we could perform. We could only calculate the size of the largest connected component in the nearest neighbor graph. For  $k = 10$ , only 28.4% of the positive examples could be reached directly, but increasing  $k$  to 100 improved that dramatically to 96.7%. For such a large connected component, one might have expected active learning to perform better in Section 4.2. By analyzing the embeddings, however, we found that examples are spread almost uniformly across the space with an average cosine similarity of 0.004. For comparison, the average cosine similarity for concepts in ImageNet and OpenImages was  $0.453 \pm 0.077$  and  $0.361 \pm 0.105$  respectively.

More generally, increasing  $k$  increased the size of the largest components and reduced the average length of the shortest path between examples. This relationship helps to explain why the gap between SEALS and the baseline approaches closes as  $k$  increases. For sufficiently large  $k$ , SEALS becomes equivalent to the baseline approaches because all examples are connected and included in the candidate pool. Nevertheless, as  $k$  and the candidate pool increase, so does the computational complexity of all of the active selection strategies. With this in mind,  $k$  allows SEALS to smoothly trade-off between the labeling efficiency of the underlying selection strategies and computational efficiency. This makes active learning and search tractable, given almost any computational budget.

## 5 Conclusion

In this work, we introduced Similarity search for Efficient Active Learning and Search (SEALS), where the candidate pool for labeling is restricted to the nearest neighbors of the currently labeled set. Across three large datasets, three selection strategies, and 604 concepts, we found that SEALS achieved similar model quality and recall of positive examples as the baseline approaches, which scan over all of the unlabeled data, while improving computational efficiency by orders of magnitude.



## Broader Impact

Our work attacks both the labeling and computational costs of machine learning and will hopefully make machine learning much more affordable. Instead of being limited to a small number of large teams and organizations with the budget to label data and the computational resources to train on it, SEALS dramatically reduces the barrier to machine learning, enabling small teams or individuals to build accurate classifiers. SEALS does, however, introduce another system component, a similarity search index, which adds some additional engineering complexity to build, tune, and maintain. Fortunately, several highly optimized implementations like Annoy <sup>2</sup> and Faiss <sup>3</sup> work reasonably well out of the box. There is a risk that poor embeddings will lead to disjointed components for a given concept. This failure mode may prevent SEALS from reaching all fragments of a concept or take a longer time to do so, as mentioned in Section 4.4. However, active learning and search methods often involve humans in the loop, which could detect biases and correct them by adding more examples.

## Acknowledgments and Disclosure of Funding

The Stanford research was supported in part by affiliate members and other supporters of the Stanford DAWN project—Ant Financial, Facebook, Google, Infosys, NEC, and VMware—as well as Toyota Research Institute, Northrop Grumman, Cisco, SAP, and the NSF under CAREER grant CNS-1651570. Any opinions, findings, and conclusions or recommendations expressed in this material are those of the authors and do not necessarily reflect the views of the National Science Foundation. Toyota Research Institute (“TRI”) provided funds to assist the authors with their research but this article solely reflects the opinions and conclusions of its authors and not TRI or any other Toyota entity.

## References

- [1] Sami Abu-El-Haija, Nisarg Kothari, Joonseok Lee, Paul Natsev, George Toderici, Balakrishnan Varadarajan, and Sudheendra Vijayanarasimhan. Youtube-8m: A large-scale video classification benchmark, 2016.
- [2] Dario Amodei and Danny Hernandez. Ai and compute, May 2018. URL <https://blog.openai.com/ai-and-compute/>.
- [3] Khalid Ashmawy, Shouheng Yi, and Alex Chao. Searchable ground truth: Querying uncommon scenarios in self-driving car development. <https://eng.uber.com/searchable-ground-truth-atg/>, 10 2019.
- [4] Jon Louis Bentley. Multidimensional binary search trees used for associative searching. *Communications of the ACM*, 18(9):509–517, 1975.
- [5] Holger Caesar, Varun Bankiti, Alex H. Lang, Sourabh Vora, Venice Erin Liong, Qiang Xu, Anush Krishnan, Yu Pan, Giancarlo Baldan, and Oscar Beijbom. nuscenes: A multimodal dataset for autonomous driving. *arXiv preprint arXiv:1903.11027*, 2019.
- [6] Moses S Charikar. Similarity estimation techniques from rounding algorithms. In *Proceedings of the thirty-fourth annual ACM symposium on Theory of computing*, pages 380–388, 2002.
- [7] Ciprian Chelba, Tomas Mikolov, Mike Schuster, Qi Ge, Thorsten Brants, Philipp Koehn, and Tony Robinson. One billion word benchmark for measuring progress in statistical language modeling. Technical report, Google, 2013. URL <http://arxiv.org/abs/1312.3005>.
- [8] Cody Coleman, Christopher Yeh, Stephen Mussmann, Baharan Mirzasoleiman, Peter Bailis, Percy Liang, Jure Leskovec, and Matei Zaharia. Selection via proxy: Efficient data selection for deep learning. In *International Conference on Learning Representations*, 2020. URL <https://openreview.net/forum?id=HJg2b0VYDr>.

---

<sup>2</sup><https://github.com/spotify/annoy>

<sup>3</sup><https://github.com/facebookresearch/faiss>

- [9] Roman Garnett, Yamuna Krishnamurthy, Xuehan Xiong, Jeff Schneider, and Richard Mann. Bayesian optimal active search and surveying. In *Proceedings of the 29th International Conference on Machine Learning*, ICML'12, page 843–850, Madison, WI, USA, 2012. Omnipress. ISBN 9781450312851.
- [10] Kaiming He, Xiangyu Zhang, Shaoqing Ren, and Jian Sun. Deep residual learning for image recognition. In *Proceedings of Conference on Computer Vision and Pattern Recognition*, 2016.
- [11] Kenneth Holstein, Jennifer Wortman Vaughan, Hal Daumé III, Miro Dudik, and Hanna Wallach. Improving fairness in machine learning systems: What do industry practitioners need? In *Proceedings of the 2019 CHI Conference on Human Factors in Computing Systems*, pages 1–16, 2019.
- [12] Shali Jiang, Gustavo Malkomes, Geoff Converse, Alyssa Shofner, Benjamin Moseley, and Roman Garnett. Efficient nonmyopic active search. In Doina Precup and Yee Whye Teh, editors, *Proceedings of the 34th International Conference on Machine Learning*, volume 70 of *Proceedings of Machine Learning Research*, pages 1714–1723, International Convention Centre, Sydney, Australia, 06–11 Aug 2017. PMLR. URL <http://proceedings.mlr.press/v70/jiang17d.html>.
- [13] Shali Jiang, Gustavo Malkomes, Matthew Abbott, Benjamin Moseley, and Roman Garnett. Efficient nonmyopic batch active search. In *Advances in Neural Information Processing Systems*, pages 1099–1109, 2018.
- [14] Shali Jiang, Roman Garnett, and Benjamin Moseley. Cost effective active search. In H. Wallach, H. Larochelle, A. Beygelzimer, F. d'Alché-Buc, E. Fox, and R. Garnett, editors, *Advances in Neural Information Processing Systems 32*, pages 4880–4889. Curran Associates, Inc., 2019. URL <http://papers.nips.cc/paper/8734-cost-effective-active-search.pdf>.
- [15] Jeff Johnson, Matthijs Douze, and Hervé Jégou. Billion-scale similarity search with gpus. *arXiv preprint arXiv:1702.08734*, 2017.
- [16] Andrej Karpathy. Train ai 2018 - building the software 2.0 stack, 2018. URL <https://vimeo.com/272696002>.
- [17] Andrej Karpathy. Ai for full-self driving, 2020. URL <https://youtu.be/hx7BXih7zx8>.
- [18] Andreas Kirsch, Joost van Amersfoort, and Yarin Gal. Batchbald: Efficient and diverse batch acquisition for deep bayesian active learning. In *Advances in Neural Information Processing Systems*, pages 7024–7035, 2019.
- [19] Alina Kuznetsova, Hassan Rom, Neil Alldrin, Jasper Uijlings, Ivan Krasin, Jordi Pont-Tuset, Shahab Kamali, Stefan Popov, Matteo Mallocci, Alexander Kolesnikov, Tom Duerig, and Vittorio Ferrari. The open images dataset v4: Unified image classification, object detection, and visual relationship detection at scale. *IJCV*, 2020.
- [20] Kevin Lee, Vijay Rao, and William Christie Arnold. Accelerating facebook's infrastructure with application-specific hardware. <https://engineering.fb.com/data-center-engineering/accelerating-infrastructure/>, 3 2019.
- [21] David D Lewis and William A Gale. A sequential algorithm for training text classifiers. In *Proceedings of the 17th annual international ACM SIGIR conference on Research and development in information retrieval*, pages 3–12. Springer-Verlag New York, Inc., 1994.
- [22] Christoph Mayer and Radu Timofte. Adversarial sampling for active learning. In *The IEEE Winter Conference on Applications of Computer Vision*, pages 3071–3079, 2020.
- [23] Robert Pinsler, Jonathan Gordon, Eric Nalisnick, and José Miguel Hernández-Lobato. Bayesian batch active learning as sparse subset approximation. In *Advances in Neural Information Processing Systems*, pages 6356–6367, 2019.

- [24] Nils Reimers and Iryna Gurevych. Sentence-BERT: Sentence embeddings using Siamese BERT-networks. In *Proceedings of the 2019 Conference on Empirical Methods in Natural Language Processing and the 9th International Joint Conference on Natural Language Processing (EMNLP-IJCNLP)*, pages 3982–3992, Hong Kong, China, November 2019. Association for Computational Linguistics. doi: 10.18653/v1/D19-1410. URL <https://www.aclweb.org/anthology/D19-1410>.
- [25] Olga Russakovsky, Jia Deng, Hao Su, Jonathan Krause, Sanjeev Satheesh, Sean Ma, Zhiheng Huang, Andrej Karpathy, Aditya Khosla, Michael Bernstein, et al. Imagenet large scale visual recognition challenge. *International journal of computer vision*, 115(3):211–252, 2015.
- [26] Ozan Sener and Silvio Savarese. Active learning for convolutional neural networks: A core-set approach. In *International Conference on Learning Representations*, 2018. URL <https://openreview.net/forum?id=H1aIuk-RW>.
- [27] Burr Settles. Active learning literature survey. Technical report, University of Wisconsin-Madison Department of Computer Sciences, 2009.
- [28] Burr Settles. From theories to queries: Active learning in practice. In Isabelle Guyon, Gavin Cawley, Gideon Dror, Vincent Lemaire, and Alexander Statnikov, editors, *Active Learning and Experimental Design workshop In conjunction with AISTATS 2010*, volume 16 of *Proceedings of Machine Learning Research*, pages 1–18, Sardinia, Italy, 16 May 2011. PMLR. URL <http://proceedings.mlr.press/v16/settles11a.html>.
- [29] Burr Settles. Active learning. *Synthesis Lectures on Artificial Intelligence and Machine Learning*, 6(1):1–114, 2012.
- [30] Burr Settles and Mark Craven. An analysis of active learning strategies for sequence labeling tasks. In *Proceedings of the Conference on Empirical Methods in Natural Language Processing, EMNLP ’08*, page 1070–1079, USA, 2008. Association for Computational Linguistics.
- [31] Bart Thomee, David A. Shamma, Gerald Friedland, Benjamin Elizalde, Karl Ni, Douglas Poland, Damian Borth, and Li-Jia Li. Yfcc100m. *Communications of the ACM*, 59(2):64–73, Jan 2016. ISSN 1557-7317. doi: 10.1145/2812802. URL <http://dx.doi.org/10.1145/2812802>.
- [32] Mengting Wan, Rishabh Misra, Ndapa Nakashole, and Julian J. McAuley. Fine-grained spoiler detection from large-scale review corpora. In Anna Korhonen, David R. Traum, and Lluís Màrquez, editors, *Proceedings of the 57th Conference of the Association for Computational Linguistics, ACL 2019, Florence, Italy, July 28- August 2, 2019, Volume 1: Long Papers*, pages 2605–2610. Association for Computational Linguistics, 2019. doi: 10.18653/v1/p19-1248. URL <https://doi.org/10.18653/v1/p19-1248>.
- [33] Manfred K Warmuth, Jun Liao, Gunnar Rätsch, Michael Mathieson, Santosh Putta, and Christian Lemmen. Active learning with support vector machines in the drug discovery process. *Journal of chemical information and computer sciences*, 43(2):667–673, 2003.
- [34] Manfred KK Warmuth, Gunnar Rätsch, Michael Mathieson, Jun Liao, and Christian Lemmen. Active learning in the drug discovery process. In *Advances in Neural information processing systems*, pages 1449–1456, 2002.
- [35] Donggeun Yoo and In So Kweon. Learning loss for active learning. In *Proceedings of the IEEE Conference on Computer Vision and Pattern Recognition*, pages 93–102, 2019.
- [36] Xiang Zhang, Junbo Zhao, and Yann LeCun. Character-level convolutional networks for text classification. In *Advances in neural information processing systems*, pages 649–657, 2015.
- [37] Jia-Jie Zhu and José Bento. Generative adversarial active learning. *arXiv preprint arXiv:1702.07956*, 2017.
- [38] Yukun Zhu, Ryan Kiros, Rich Zemel, Ruslan Salakhutdinov, Raquel Urtasun, Antonio Torralba, and Sanja Fidler. Aligning books and movies: Towards story-like visual explanations by watching movies and reading books. In *Proceedings of the IEEE international conference on computer vision*, pages 19–27, 2015.

## Supplementary Material

### Number of initial positives

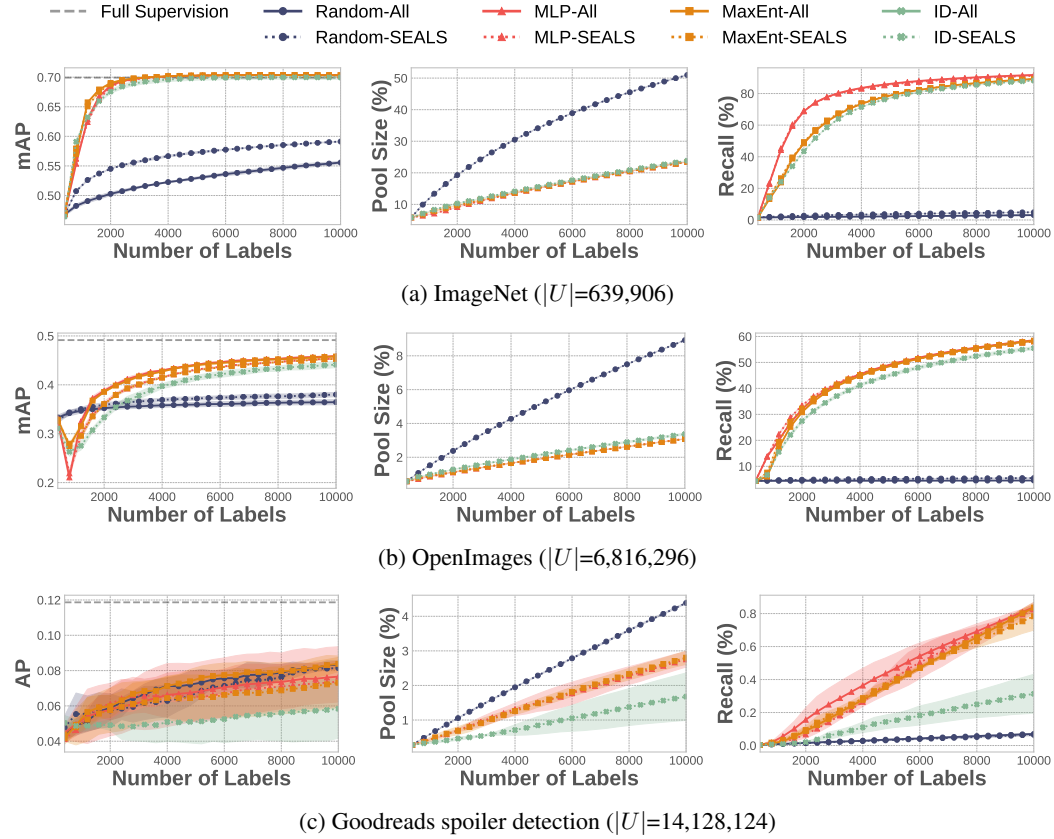


Figure 3: **Active learning and search with 20 positive seed examples** and a labeling budget of 10,000 examples on ImageNet (top), OpenImages (center), and Goodreads (bottom). Across datasets and strategies, SEALS with  $k = 100$  performs similarly to the baseline approach in terms of both the error the model achieves for active learning (left) and the recall of positive examples for active search (right), while only considering a fraction of the unlabeled data  $U$  (middle).

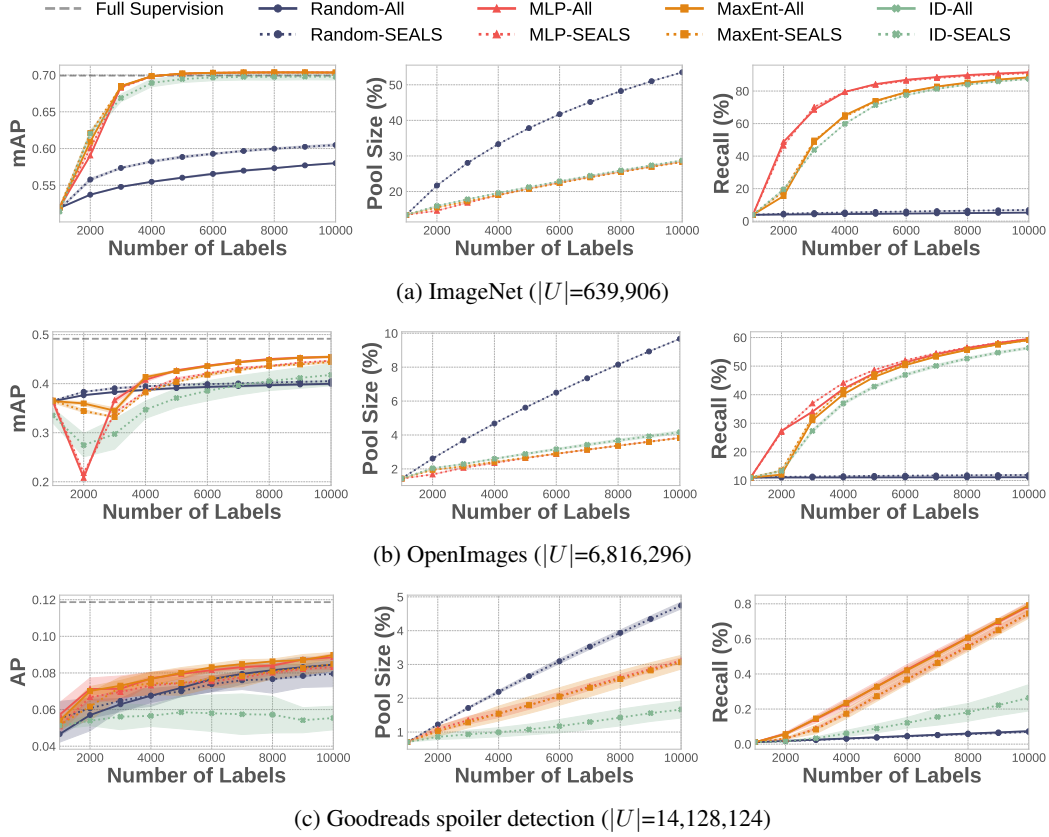


Figure 4: **Active learning and search with 50 positive seed examples** and a labeling budget of 10,000 examples on ImageNet (top), OpenImages (center), and Goodreads (bottom). Across datasets and strategies, SEALS with  $k = 100$  performs similarly to the baseline approach in terms of both the error the model achieves for active learning (left) and the recall of positive examples for active search (right), while only considering a fraction of the unlabeled data  $U$  (middle).

#### Labeling budget of 100,000 examples for Goodreads spoiler detection

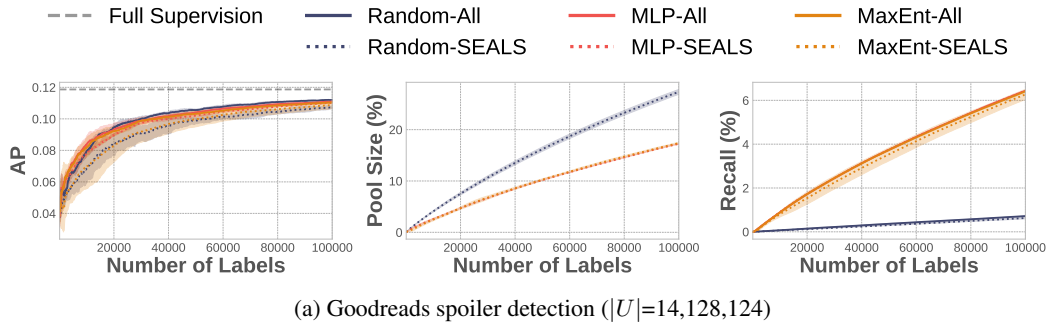


Figure 5: **Active learning and search with a labeling budget of 100,000 examples on Goodreads.** Across datasets and strategies, SEALS with  $k = 100$  performs similarly to the baseline approach in terms of both the error the model achieves for active learning (left) and the recall of positive examples for active search (right), while only considering a fraction of the data  $U$  (middle). Despite the larger labeling budget, all the selection strategies performed similarly to random sampling for active learning, as in Figure 1. For active search, MaxEnt and MLP continue to improve recall. ID was excluded because of the growing pool size and computation.

## Impact of $k$ on SEALS

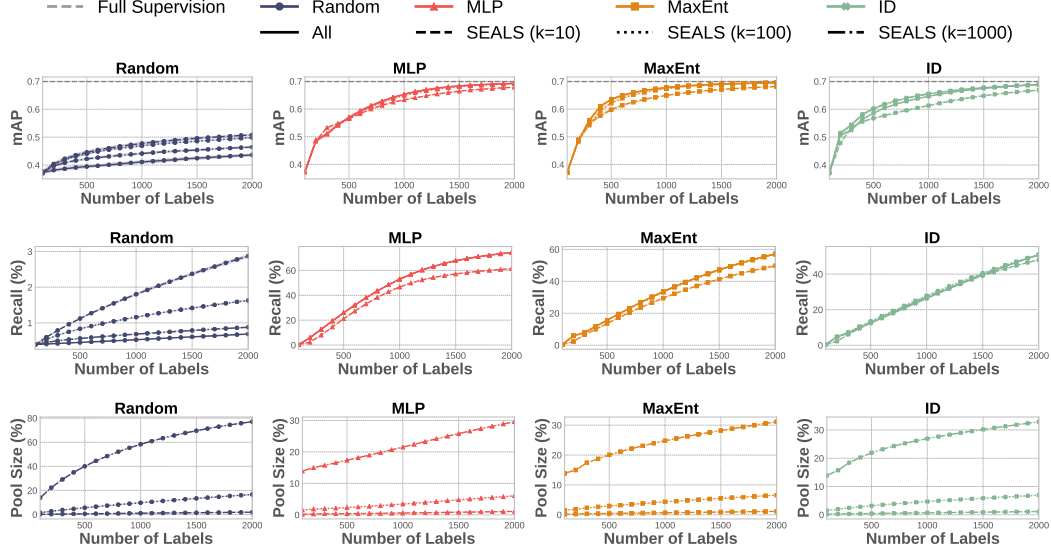


Figure 6: **Impact of increasing  $k$  on ImageNet ( $|U|=639,906$ ).** Larger values of  $k$  help to close the gap between SEALS and the baseline approach that considers all of the unlabeled data for both active learning (top) and active search (middle). However, increasing  $k$  also increases the candidate pool size (bottom), presenting a trade-off between labeling efficiency and computational efficiency.

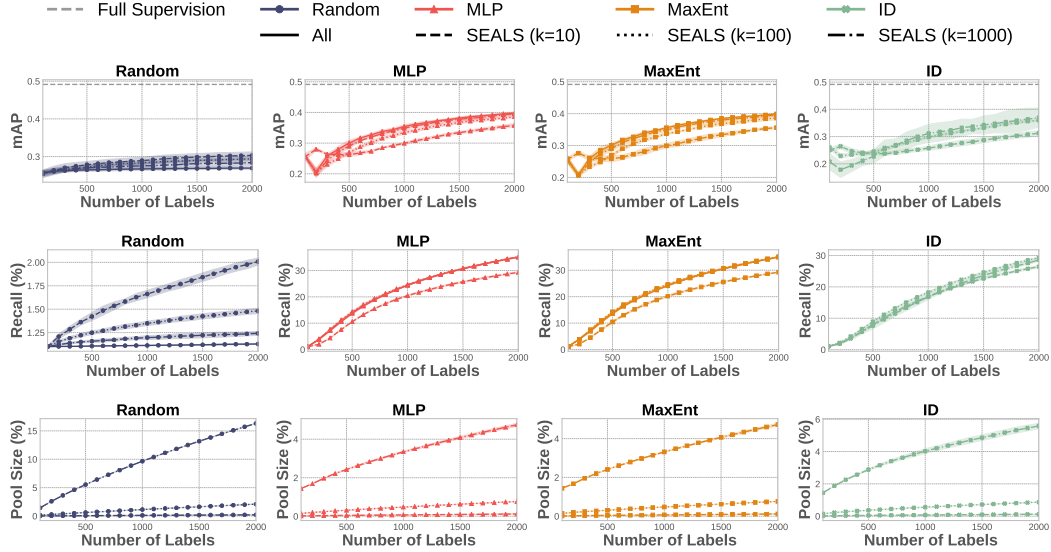


Figure 7: **Impact of increasing  $k$  on OpenImages ( $|U|=6,816,296$ ).** Larger values of  $k$  help to close the gap between SEALS and the baseline approach that considers all of the unlabeled data for both active learning (top) and active search (middle). However, increasing  $k$  also increases the candidate pool size (bottom), presenting a trade-off between labeling efficiency and computational efficiency.

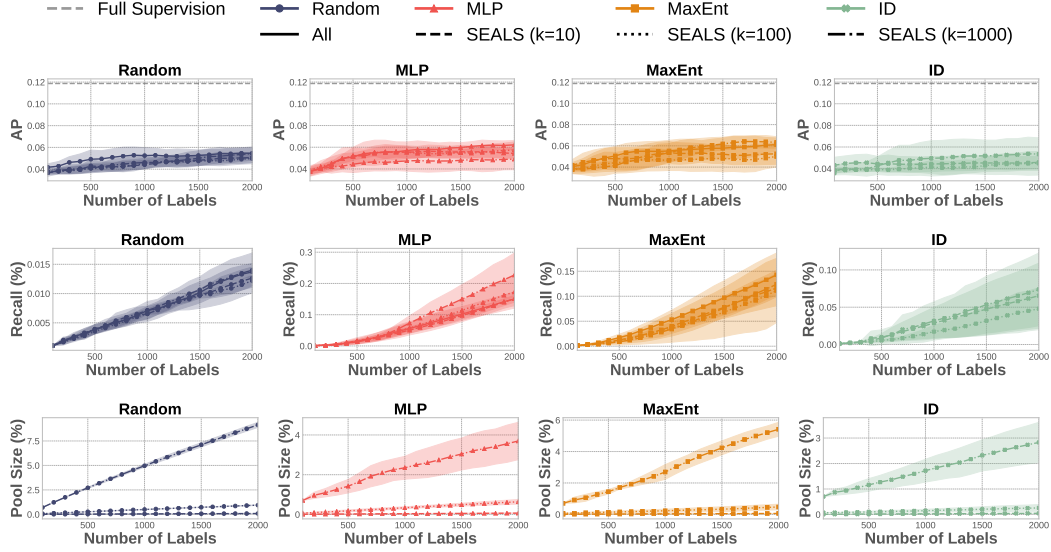


Figure 8: **Impact of increasing  $k$  on Goodreads spoiler detection ( $|U|=14,128,124$ ).** Unlike ImageNet (Figure 6) and OpenImages (Figure 7), SEALS and the base approach perform similarly regardless of  $k$  for both active learning (top) and active search (middle). As mentioned in Section 4.4, spoilers are spread almost uniformly across the space with an average cosine similarity of 0.004, meaning there is less latent structure to exploit and the  $k$ -nearest neighbor graph is less critical.

## Active learning on each selected class from OpenImages

Table 3: **Top  $\frac{1}{3}$  of classes from Openimages for active learning.** (1 of 3) Average precision for each selected class (153 total) from OpenImages with a labeling budget of 2,000 examples. Classes are in descending order based on the performance gain of MaxEnt-SEALS over Random-All.

Label Name	Display Name	Total Positives	Random (All)	MaxEnt (SEALS)	MaxEnt (All)	Full Supervision
/m/018gpn	Hurdling	269	0.26 $\pm$ 0.094	0.80 $\pm$ 0.005	0.79 $\pm$ 0.005	0.80
/m/0dqb5	Citrus	796	0.34 $\pm$ 0.191	0.87 $\pm$ 0.001	0.87 $\pm$ 0.003	0.87
/m/0btmb	Superhero	968	0.17 $\pm$ 0.106	0.70 $\pm$ 0.008	0.70 $\pm$ 0.021	0.67
/m/09wzfj	California roll	368	0.05 $\pm$ 0.018	0.56 $\pm$ 0.007	0.56 $\pm$ 0.007	0.58
/m/01xc8d	Rope	618	0.29 $\pm$ 0.243	0.80 $\pm$ 0.003	0.81 $\pm$ 0.003	0.74
/m/0111f78	Shrimp	907	0.07 $\pm$ 0.024	0.56 $\pm$ 0.002	0.56 $\pm$ 0.009	0.58
/m/0910j_	Ring	676	0.15 $\pm$ 0.029	0.61 $\pm$ 0.012	0.64 $\pm$ 0.018	0.64
/m/0dwxr	Modern pentathlon	772	0.13 $\pm$ 0.085	0.58 $\pm$ 0.010	0.47 $\pm$ 0.257	0.51
/m/02yhp1	San Pedro cactus	318	0.17 $\pm$ 0.114	0.62 $\pm$ 0.003	0.63 $\pm$ 0.005	0.71
/m/0bpn3c2	Skateboarding Equipment	862	0.20 $\pm$ 0.105	0.62 $\pm$ 0.073	0.66 $\pm$ 0.013	0.66
/m/0cyz6w	Whole food	708	0.18 $\pm$ 0.115	0.58 $\pm$ 0.020	0.60 $\pm$ 0.020	0.57
/m/01943w	Ibis	259	0.29 $\pm$ 0.068	0.68 $\pm$ 0.010	0.69 $\pm$ 0.009	0.66
/m/03d8m_	Monster truck	286	0.41 $\pm$ 0.124	0.79 $\pm$ 0.010	0.80 $\pm$ 0.004	0.81
/m/01s0ps	Electric piano	345	0.24 $\pm$ 0.106	0.61 $\pm$ 0.024	0.60 $\pm$ 0.020	0.48
/m/01cz4w	Bilberry	228	0.10 $\pm$ 0.091	0.45 $\pm$ 0.031	0.45 $\pm$ 0.026	0.32
/m/0j_5b	Monoplane	756	0.13 $\pm$ 0.072	0.48 $\pm$ 0.014	0.43 $\pm$ 0.174	0.48
/m/058qzx	Kitchen knife	360	0.32 $\pm$ 0.130	0.66 $\pm$ 0.003	0.65 $\pm$ 0.004	0.66
/m/0cghn	Mcdonnell douglas f/a-18 hornet	160	0.11 $\pm$ 0.065	0.44 $\pm$ 0.041	0.47 $\pm$ 0.027	0.37
/m/05z55	Pasta	954	0.42 $\pm$ 0.104	0.75 $\pm$ 0.014	0.75 $\pm$ 0.007	0.79
/m/05h5q_s	Glider	393	0.08 $\pm$ 0.045	0.40 $\pm$ 0.004	0.40 $\pm$ 0.004	0.48
/m/026545k	Elk	353	0.15 $\pm$ 0.018	0.46 $\pm$ 0.014	0.48 $\pm$ 0.005	0.45
/m/0dxb5	Berry	874	0.30 $\pm$ 0.117	0.61 $\pm$ 0.007	0.61 $\pm$ 0.007	0.69
/m/01ngsj	Daylily	391	0.20 $\pm$ 0.077	0.51 $\pm$ 0.006	0.50 $\pm$ 0.003	0.49
/m/0413lm	Shooting range	189	0.38 $\pm$ 0.127	0.69 $\pm$ 0.011	0.69 $\pm$ 0.008	0.68
/m/0wgq98_	Skating	561	0.17 $\pm$ 0.017	0.48 $\pm$ 0.028	0.43 $\pm$ 0.147	0.40
/m/01xq0k1	Cattle	5995	0.37 $\pm$ 0.085	0.67 $\pm$ 0.007	0.68 $\pm$ 0.006	0.74
/m/0cfk35	Chocolate truffle	288	0.10 $\pm$ 0.047	0.39 $\pm$ 0.015	0.40 $\pm$ 0.020	0.42
/m/0cnxs6x	Tooth	976	0.16 $\pm$ 0.053	0.44 $\pm$ 0.069	0.48 $\pm$ 0.074	0.56
/m/01111r	Briefs	539	0.15 $\pm$ 0.074	0.43 $\pm$ 0.008	0.44 $\pm$ 0.005	0.46
/m/04fyb1	Sirloin steak	297	0.14 $\pm$ 0.092	0.42 $\pm$ 0.007	0.42 $\pm$ 0.032	0.46
/m/0cl6l	Straw	547	0.33 $\pm$ 0.142	0.61 $\pm$ 0.004	0.62 $\pm$ 0.011	0.61
/m/06lk1	Rat	1151	0.32 $\pm$ 0.098	0.60 $\pm$ 0.003	0.60 $\pm$ 0.003	0.61
/m/03fwl	Goat	1190	0.17 $\pm$ 0.056	0.44 $\pm$ 0.017	0.45 $\pm$ 0.019	0.61
/m/033cnk	Egg (Food)	1193	0.14 $\pm$ 0.089	0.40 $\pm$ 0.061	0.37 $\pm$ 0.019	0.63
/m/058hry	Smoothie	330	0.15 $\pm$ 0.039	0.41 $\pm$ 0.007	0.41 $\pm$ 0.004	0.38
/m/020dp	Cranberry	450	0.13 $\pm$ 0.099	0.39 $\pm$ 0.041	0.39 $\pm$ 0.012	0.37
/m/0h8n982	Shelving	810	0.27 $\pm$ 0.097	0.53 $\pm$ 0.012	0.53 $\pm$ 0.013	0.51
/m/01bmhj	Thumb	895	0.07 $\pm$ 0.133	0.32 $\pm$ 0.178	0.39 $\pm$ 0.043	0.41
/m/0cnmr	Fur	834	0.08 $\pm$ 0.087	0.33 $\pm$ 0.013	0.33 $\pm$ 0.016	0.31
/m/0g9vs81	Steamed rice	580	0.10 $\pm$ 0.055	0.35 $\pm$ 0.039	0.37 $\pm$ 0.032	0.48
/m/0176mf	Belt	467	0.06 $\pm$ 0.035	0.29 $\pm$ 0.018	0.31 $\pm$ 0.005	0.31
/m/0335ws	Concert dance	357	0.37 $\pm$ 0.096	0.60 $\pm$ 0.019	0.60 $\pm$ 0.020	0.70
/m/05h35z	Formula racing	351	0.33 $\pm$ 0.142	0.55 $\pm$ 0.027	0.54 $\pm$ 0.048	0.60
/m/011lx7	Bracelet	770	0.09 $\pm$ 0.082	0.31 $\pm$ 0.042	0.33 $\pm$ 0.020	0.24
/m/025sv9y	Landscaping	789	0.26 $\pm$ 0.113	0.48 $\pm$ 0.120	0.51 $\pm$ 0.065	0.63
/m/02qfx	Embroidery	356	0.32 $\pm$ 0.044	0.53 $\pm$ 0.003	0.53 $\pm$ 0.016	0.60
/m/019ctc	Galleon	182	0.45 $\pm$ 0.028	0.66 $\pm$ 0.005	0.66 $\pm$ 0.007	0.61
/m/03lnzv	Calabaza	870	0.50 $\pm$ 0.189	0.71 $\pm$ 0.025	0.75 $\pm$ 0.014	0.81
/m/02zfvv	American shorthair	2084	0.12 $\pm$ 0.047	0.32 $\pm$ 0.033	0.32 $\pm$ 0.038	0.24
/m/01ckgp	Interaction	924	0.04 $\pm$ 0.036	0.24 $\pm$ 0.058	0.25 $\pm$ 0.140	0.37
/m/011b5	Chess	740	0.53 $\pm$ 0.165	0.73 $\pm$ 0.007	0.74 $\pm$ 0.009	0.86



Table 4: **Middle  $\frac{1}{3}$  of classes from Openimages for active learning.** (2 of 3) Average precision for each selected class (153 total) from OpenImages with a labeling budget of 2,000 examples. Classes are in descending order based on the performance gain of MaxEnt-SEALS over Random-All.

Label Name	Display Name	Total Positives	Random (All)	MaxEnt (SEALS)	MaxEnt (All)	Full Supervision
/m/04s5jq	Costume design	818	0.07 $\pm$ 0.060	0.26 $\pm$ 0.015	0.26 $\pm$ 0.019	0.28
/m/02n7rn	Paddy field	468	0.17 $\pm$ 0.056	0.36 $\pm$ 0.009	0.36 $\pm$ 0.011	0.43
/m/05mfbz	Optical instrument	649	0.15 $\pm$ 0.071	0.33 $\pm$ 0.066	0.33 $\pm$ 0.024	0.28
/m/01n5cy	Carpet	644	0.05 $\pm$ 0.049	0.23 $\pm$ 0.134	0.28 $\pm$ 0.122	0.43
/m/02hnl	Drums	741	0.52 $\pm$ 0.158	0.70 $\pm$ 0.012	0.72 $\pm$ 0.010	0.83
/m/0385k	Gymnast	235	0.39 $\pm$ 0.070	0.57 $\pm$ 0.009	0.59 $\pm$ 0.005	0.65
/m/0f70b4	Seafood boil	322	0.31 $\pm$ 0.081	0.48 $\pm$ 0.002	0.49 $\pm$ 0.003	0.51
/m/0hp3n	Pavlova	195	0.19 $\pm$ 0.051	0.36 $\pm$ 0.008	0.36 $\pm$ 0.006	0.34
/m/0fd2m	Deacon	341	0.48 $\pm$ 0.057	0.64 $\pm$ 0.010	0.64 $\pm$ 0.008	0.67
/m/03f0h4	Roman temple	345	0.63 $\pm$ 0.037	0.79 $\pm$ 0.004	0.79 $\pm$ 0.001	0.82
/m/0cfdh	Maple	2301	0.06 $\pm$ 0.043	0.22 $\pm$ 0.052	0.21 $\pm$ 0.014	0.36
/m/07h51	Trail riding	679	0.21 $\pm$ 0.031	0.37 $\pm$ 0.015	0.37 $\pm$ 0.002	0.38
/m/0168g6	Factory	333	0.17 $\pm$ 0.070	0.33 $\pm$ 0.011	0.34 $\pm$ 0.009	0.35
/m/01y2w	Ciconiiformes	426	0.33 $\pm$ 0.066	0.49 $\pm$ 0.012	0.51 $\pm$ 0.012	0.48
/m/0hqkz	Grapefruit	506	0.50 $\pm$ 0.062	0.65 $\pm$ 0.003	0.65 $\pm$ 0.003	0.69
/m/0642b4	Cupboard	898	0.53 $\pm$ 0.155	0.68 $\pm$ 0.007	0.69 $\pm$ 0.007	0.75
/m/03931h	Stele	450	0.12 $\pm$ 0.074	0.26 $\pm$ 0.021	0.25 $\pm$ 0.028	0.35
/m/0cl3b	Rye	128	0.51 $\pm$ 0.058	0.64 $\pm$ 0.009	0.64 $\pm$ 0.007	0.65
/m/0jhv_	Blackberry	245	0.67 $\pm$ 0.062	0.80 $\pm$ 0.001	0.80 $\pm$ 0.001	0.79
/m/02zg0m	Chartreux	147	0.50 $\pm$ 0.088	0.63 $\pm$ 0.005	0.63 $\pm$ 0.005	0.69
/m/03c5wm	Cargo ship	219	0.70 $\pm$ 0.134	0.83 $\pm$ 0.003	0.83 $\pm$ 0.002	0.86
/m/0gv1x	Parrot	1546	0.59 $\pm$ 0.085	0.72 $\pm$ 0.016	0.76 $\pm$ 0.039	0.92
/m/03vd46	Herd	648	0.42 $\pm$ 0.200	0.54 $\pm$ 0.010	0.55 $\pm$ 0.010	0.67
/m/07x7yj	Pancit	385	0.21 $\pm$ 0.045	0.33 $\pm$ 0.011	0.33 $\pm$ 0.007	0.31
/m/025_v	Cactus	377	0.05 $\pm$ 0.021	0.17 $\pm$ 0.008	0.18 $\pm$ 0.011	0.22
/m/01j3sz	Laugh	750	0.06 $\pm$ 0.039	0.18 $\pm$ 0.074	0.17 $\pm$ 0.043	0.26
/m/02zkn_	Log cabin	448	0.44 $\pm$ 0.050	0.55 $\pm$ 0.006	0.55 $\pm$ 0.004	0.62
/m/01fyrh	Downhill	194	0.42 $\pm$ 0.065	0.53 $\pm$ 0.011	0.51 $\pm$ 0.003	0.59
/m/04y4h8h	Bathroom cabinet	368	0.29 $\pm$ 0.061	0.40 $\pm$ 0.005	0.39 $\pm$ 0.007	0.37
/m/079bkr	Mode of transport	1387	0.15 $\pm$ 0.232	0.26 $\pm$ 0.161	0.16 $\pm$ 0.155	0.54
/m/01jnzj	Construction	515	0.13 $\pm$ 0.075	0.23 $\pm$ 0.012	0.26 $\pm$ 0.018	0.34
/m/02qm2x	Icing	1118	0.13 $\pm$ 0.054	0.23 $\pm$ 0.033	0.25 $\pm$ 0.021	0.46
/m/0dlgz	Bakmi	191	0.27 $\pm$ 0.042	0.37 $\pm$ 0.021	0.37 $\pm$ 0.013	0.36
/m/09l65	Singer	604	0.12 $\pm$ 0.050	0.21 $\pm$ 0.067	0.21 $\pm$ 0.033	0.40
/m/076t48l	Coral reef fish	434	0.51 $\pm$ 0.137	0.60 $\pm$ 0.007	0.64 $\pm$ 0.005	0.79
/m/01295w	Galliformes	674	0.72 $\pm$ 0.071	0.80 $\pm$ 0.016	0.82 $\pm$ 0.026	0.92
/m/0frq6	Pork	464	0.06 $\pm$ 0.029	0.14 $\pm$ 0.008	0.14 $\pm$ 0.006	0.15
/m/0dvg9	Ancient roman architecture	589	0.61 $\pm$ 0.109	0.68 $\pm$ 0.006	0.70 $\pm$ 0.007	0.77
/m/01wkk9	Town square	617	0.31 $\pm$ 0.067	0.38 $\pm$ 0.016	0.36 $\pm$ 0.023	0.47
/m/01_6hg	Delicatessen	196	0.14 $\pm$ 0.071	0.21 $\pm$ 0.010	0.22 $\pm$ 0.010	0.27
/m/03vtj	Ice	682	0.23 $\pm$ 0.082	0.30 $\pm$ 0.057	0.32 $\pm$ 0.009	0.55
/m/02r0zt	White-tailed deer	238	0.34 $\pm$ 0.015	0.40 $\pm$ 0.028	0.43 $\pm$ 0.014	0.43
/m/0hr8	Asphalt	1026	0.23 $\pm$ 0.124	0.29 $\pm$ 0.026	0.29 $\pm$ 0.021	0.45
/m/0b97cn	Lamian	257	0.23 $\pm$ 0.139	0.29 $\pm$ 0.016	0.32 $\pm$ 0.016	0.28
/m/0jqb	Annual plant	677	0.39 $\pm$ 0.066	0.44 $\pm$ 0.037	0.43 $\pm$ 0.043	0.58
/m/019mbd	Antenna	545	0.10 $\pm$ 0.040	0.14 $\pm$ 0.005	0.13 $\pm$ 0.004	0.29
/m/03jqf3	Chevrolet silverado	115	0.05 $\pm$ 0.020	0.09 $\pm$ 0.012	0.08 $\pm$ 0.003	0.12
/m/09q2t	Brown	1427	0.02 $\pm$ 0.003	0.05 $\pm$ 0.044	0.07 $\pm$ 0.069	0.20
/m/06wqb	Space	1006	0.03 $\pm$ 0.012	0.06 $\pm$ 0.029	0.03 $\pm$ 0.044	0.14
/m/01c34b	Flooring	814	0.10 $\pm$ 0.010	0.13 $\pm$ 0.007	0.14 $\pm$ 0.003	0.20
/m/0hlw	Algae	426	0.15 $\pm$ 0.063	0.18 $\pm$ 0.004	0.19 $\pm$ 0.005	0.26

Table 5: **Bottom  $\frac{1}{3}$  of classes from Openimages for active learning.** (3 of 3) Average precision for each selected class (153 total) from OpenImages with a labeling budget of 2,000 examples. Classes are in descending order based on the performance gain of MaxEnt-SEALS over Random-All.

Label Name	Display Name	Total Positives	Random (All)	MaxEnt (SEALS)	MaxEnt (All)	Full Supervision
/m/01jfm_	Vehicle registration plate	5697	0.28 $\pm$ 0.066	0.31 $\pm$ 0.031	0.33 $\pm$ 0.048	0.53
/m/09qkx	Boardsport	673	0.26 $\pm$ 0.038	0.29 $\pm$ 0.011	0.29 $\pm$ 0.006	0.53
/m/0322v8	Lugger	103	0.35 $\pm$ 0.108	0.37 $\pm$ 0.005	0.37 $\pm$ 0.016	0.42
/m/03tqj	Icon	186	0.05 $\pm$ 0.045	0.07 $\pm$ 0.045	0.07 $\pm$ 0.064	0.16
/m/05nnm	Organism	1148	0.05 $\pm$ 0.041	0.07 $\pm$ 0.062	0.13 $\pm$ 0.078	0.26
/m/02mk9	Engine	656	0.16 $\pm$ 0.046	0.17 $\pm$ 0.013	0.17 $\pm$ 0.008	0.26
/m/0c0ygc	Stallion	598	0.32 $\pm$ 0.126	0.33 $\pm$ 0.025	0.40 $\pm$ 0.032	0.64
/m/01czv3	Fortification	287	0.43 $\pm$ 0.050	0.44 $\pm$ 0.025	0.46 $\pm$ 0.015	0.52
/m/03hcy1d	Mitsubishi	511	0.01 $\pm$ 0.003	0.02 $\pm$ 0.003	0.02 $\pm$ 0.007	0.04
/m/083jv	White	1494	0.02 $\pm$ 0.007	0.03 $\pm$ 0.021	0.01 $\pm$ 0.003	0.10
/m/07k1x	Tool	1549	0.08 $\pm$ 0.016	0.09 $\pm$ 0.009	0.10 $\pm$ 0.008	0.13
/m/0114_3	Bowed string instrument	728	0.72 $\pm$ 0.111	0.72 $\pm$ 0.007	0.74 $\pm$ 0.003	0.79
/m/026yps0	East-european shepherd	206	0.61 $\pm$ 0.052	0.61 $\pm$ 0.001	0.62 $\pm$ 0.003	0.65
/m/03jvv0	Teal	975	0.01 $\pm$ 0.005	0.01 $\pm$ 0.003	0.01 $\pm$ 0.001	0.04
/m/0fq22vb	Exhibition	513	0.03 $\pm$ 0.032	0.02 $\pm$ 0.002	0.02 $\pm$ 0.003	0.14
/m/02vwbzz	Electric blue	1180	0.01 $\pm$ 0.007	0.00 $\pm$ 0.002	0.01 $\pm$ 0.002	0.06
/m/01pvk	Canal	726	0.22 $\pm$ 0.077	0.21 $\pm$ 0.023	0.26 $\pm$ 0.006	0.46
/m/0641k	Paper	969	0.16 $\pm$ 0.084	0.15 $\pm$ 0.056	0.14 $\pm$ 0.062	0.41
/m/01w5c_	Aerial photography	931	0.39 $\pm$ 0.019	0.37 $\pm$ 0.018	0.37 $\pm$ 0.015	0.66
/m/0gd2v	Marine mammal	2954	0.19 $\pm$ 0.041	0.16 $\pm$ 0.014	0.15 $\pm$ 0.008	0.21
/m/0br7j6	Pleurotus eryngii	140	0.11 $\pm$ 0.024	0.08 $\pm$ 0.009	0.08 $\pm$ 0.006	0.14
/m/01rh7y	Scale model	667	0.05 $\pm$ 0.052	0.02 $\pm$ 0.003	0.02 $\pm$ 0.003	0.13
/m/01cv4r	Temperate coniferous forest	328	0.30 $\pm$ 0.050	0.26 $\pm$ 0.016	0.29 $\pm$ 0.025	0.40
/m/013y0j	Organ (Biology)	1156	0.23 $\pm$ 0.096	0.19 $\pm$ 0.095	0.07 $\pm$ 0.091	0.44
/m/033kf	Frost	483	0.20 $\pm$ 0.123	0.15 $\pm$ 0.128	0.21 $\pm$ 0.144	0.47
/m/023bbt	Wilderness	1225	0.29 $\pm$ 0.105	0.23 $\pm$ 0.125	0.24 $\pm$ 0.064	0.39
/m/09qqq	Wall	1218	0.11 $\pm$ 0.051	0.05 $\pm$ 0.015	0.05 $\pm$ 0.031	0.27
/m/05qjc	Performing arts	1030	0.12 $\pm$ 0.045	0.05 $\pm$ 0.020	0.06 $\pm$ 0.035	0.53
/m/02pkr5	Plumbing fixture	2124	0.31 $\pm$ 0.025	0.24 $\pm$ 0.019	0.27 $\pm$ 0.019	0.38
/m/038t8_	Estate	667	0.47 $\pm$ 0.050	0.39 $\pm$ 0.029	0.40 $\pm$ 0.006	0.54
/m/04rd7	Mural	649	0.13 $\pm$ 0.018	0.05 $\pm$ 0.025	0.07 $\pm$ 0.029	0.34
/m/0hkvx	Prairie	792	0.37 $\pm$ 0.074	0.29 $\pm$ 0.032	0.26 $\pm$ 0.045	0.57
/m/01d0z1	Shorebird	234	0.32 $\pm$ 0.053	0.23 $\pm$ 0.008	0.26 $\pm$ 0.003	0.37
/m/03nxtz	Cottage	670	0.36 $\pm$ 0.214	0.26 $\pm$ 0.016	0.36 $\pm$ 0.025	0.61
/m/012sbd	Tournament	841	0.15 $\pm$ 0.012	0.05 $\pm$ 0.031	0.07 $\pm$ 0.049	0.16
/m/01dv4h	Portrait	2510	0.23 $\pm$ 0.013	0.13 $\pm$ 0.076	0.18 $\pm$ 0.104	0.43
/m/01f4td	Rural area	921	0.33 $\pm$ 0.068	0.22 $\pm$ 0.052	0.28 $\pm$ 0.042	0.50
/m/0j6jq	Floodplain	567	0.61 $\pm$ 0.164	0.47 $\pm$ 0.048	0.52 $\pm$ 0.037	0.66
/m/047fr	Knitting	409	0.61 $\pm$ 0.034	0.46 $\pm$ 0.025	0.50 $\pm$ 0.006	0.73
/m/0h8ls87	Automotive exterior	1060	0.65 $\pm$ 0.122	0.49 $\pm$ 0.139	0.54 $\pm$ 0.049	0.69
/m/0541p	Multimedia	741	0.45 $\pm$ 0.104	0.29 $\pm$ 0.029	0.31 $\pm$ 0.022	0.53
/m/04qgp	Liqueur	539	0.26 $\pm$ 0.020	0.09 $\pm$ 0.007	0.14 $\pm$ 0.035	0.38
/m/0krfg	Meal	1250	0.52 $\pm$ 0.057	0.32 $\pm$ 0.074	0.38 $\pm$ 0.045	0.59
/m/099md	Soldier	1032	0.62 $\pm$ 0.087	0.40 $\pm$ 0.029	0.41 $\pm$ 0.026	0.72
/m/02mwzg	Plateau	452	0.41 $\pm$ 0.047	0.18 $\pm$ 0.010	0.24 $\pm$ 0.022	0.46
/m/01d7ng	Pelecaniformes	457	0.30 $\pm$ 0.122	0.07 $\pm$ 0.015	0.09 $\pm$ 0.006	0.32
/m/02mnkq	Bumper	985	0.49 $\pm$ 0.088	0.25 $\pm$ 0.048	0.38 $\pm$ 0.047	0.64
/m/03s7w_	Cirque	347	0.43 $\pm$ 0.069	0.15 $\pm$ 0.113	0.40 $\pm$ 0.148	0.55
/m/019cfy	Stadium	1654	0.35 $\pm$ 0.040	0.06 $\pm$ 0.020	0.10 $\pm$ 0.037	0.48
/m/0f6x8	Bird of prey	712	0.76 $\pm$ 0.087	0.40 $\pm$ 0.090	0.50 $\pm$ 0.127	0.91
/m/01sgl	Cycling	794	0.53 $\pm$ 0.054	0.13 $\pm$ 0.107	0.28 $\pm$ 0.142	0.66

### Active search on each selected class from OpenImages

Table 6: **Top  $\frac{1}{3}$  of classes from Openimages for active search.** (1 of 3) Recall (%) of positives for each selected class (153 total) from OpenImages with a labeling budget of 2,000 examples. Classes are in descending order based on the performance gain of MLP-SEALS over Random-All.

Label Name	Display Name	Total Positives	Random (All)	MLP (SEALS)	MLP (All)
/m/01943w	Ibis	259	$2.0 \pm 0.17$	$83.9 \pm 0.75$	$83.9 \pm 0.80$
/m/018gpn	Hurdling	269	$1.9 \pm 0.00$	$83.5 \pm 0.33$	$86.2 \pm 0.37$
/m/02zg0m	Chartreux	147	$3.5 \pm 0.30$	$83.9 \pm 0.37$	$84.6 \pm 0.78$
/m/026yps0	East-european shepherd	206	$2.4 \pm 0.00$	$78.2 \pm 0.59$	$78.3 \pm 0.43$
/m/04y4h8h	Bathroom cabinet	368	$1.4 \pm 0.12$	$76.8 \pm 0.35$	$77.1 \pm 0.23$
/m/0jhv_	Blackberry	245	$2.0 \pm 0.00$	$77.5 \pm 0.45$	$78.5 \pm 0.74$
/m/06lk1	Rat	1151	$0.5 \pm 0.08$	$75.1 \pm 0.16$	$75.2 \pm 0.26$
/m/026545k	Elk	353	$1.5 \pm 0.16$	$73.4 \pm 0.31$	$74.3 \pm 0.81$
/m/0cl3b	Rye	128	$3.9 \pm 0.00$	$74.7 \pm 1.18$	$74.5 \pm 1.52$
/m/0f70b4	Seafood boil	322	$1.6 \pm 0.00$	$70.4 \pm 0.42$	$70.6 \pm 0.52$
/m/0hp3n	Pavlova	195	$2.6 \pm 0.00$	$70.8 \pm 0.36$	$71.3 \pm 0.96$
/m/03f0h4	Roman temple	345	$1.5 \pm 0.13$	$69.2 \pm 0.53$	$68.3 \pm 0.70$
/m/03d8m_	Monster truck	286	$1.7 \pm 0.00$	$68.1 \pm 0.76$	$67.8 \pm 0.52$
/m/01fyrh	Downhill	194	$2.6 \pm 0.00$	$67.2 \pm 0.59$	$69.0 \pm 0.23$
/m/01d0z1	Shorebird	234	$2.1 \pm 0.00$	$66.8 \pm 0.56$	$66.4 \pm 0.38$
/m/02yhp1	San Pedro cactus	318	$1.6 \pm 0.14$	$65.8 \pm 0.41$	$64.9 \pm 0.28$
/m/09wzfj	California roll	368	$1.4 \pm 0.12$	$65.3 \pm 0.49$	$68.0 \pm 0.12$
/m/0cgghn	Mcdonnell douglas f/a-18 hornet	160	$3.2 \pm 0.28$	$66.0 \pm 5.67$	$67.9 \pm 5.35$
/m/0br7j6	Pleurotus eryngii	140	$3.6 \pm 0.00$	$65.7 \pm 1.43$	$66.1 \pm 1.08$
/m/0385k	Gymnast	235	$2.2 \pm 0.19$	$64.0 \pm 0.65$	$64.0 \pm 0.71$
/m/019ctc	Galleon	182	$2.7 \pm 0.00$	$62.4 \pm 0.92$	$61.5 \pm 1.35$
/m/07h51	Trail riding	679	$0.8 \pm 0.08$	$59.7 \pm 0.51$	$60.7 \pm 0.47$
/m/03c5wm	Cargo ship	219	$2.3 \pm 0.00$	$61.1 \pm 0.75$	$61.7 \pm 0.60$
/m/0hqkz	Grapefruit	506	$1.0 \pm 0.09$	$59.4 \pm 0.27$	$60.4 \pm 0.33$
/m/01ngsj	Daylily	391	$1.3 \pm 0.11$	$59.4 \pm 0.80$	$59.5 \pm 1.01$
/m/01cz4w	Bilberry	228	$2.2 \pm 0.00$	$58.9 \pm 1.93$	$55.2 \pm 2.31$
/m/058hry	Smoothie	330	$1.5 \pm 0.00$	$58.0 \pm 1.30$	$59.8 \pm 0.78$
/m/02qfx	Embroidery	356	$1.5 \pm 0.13$	$57.6 \pm 0.61$	$57.2 \pm 1.04$
/m/0fd2m	Deacon	341	$1.5 \pm 0.13$	$57.1 \pm 0.79$	$57.9 \pm 0.44$
/m/05h5q_s	Glider	393	$1.3 \pm 0.00$	$55.8 \pm 0.82$	$57.6 \pm 0.95$
/m/0413lm	Shooting range	189	$2.6 \pm 0.00$	$56.3 \pm 1.43$	$55.6 \pm 3.45$
/m/02r0zt	White-tailed deer	238	$2.2 \pm 0.19$	$55.8 \pm 1.50$	$55.9 \pm 1.73$
/m/076t48l	Coral reef fish	434	$1.3 \pm 0.21$	$54.8 \pm 0.75$	$54.9 \pm 0.41$
/m/07x7yj	Pancit	385	$1.3 \pm 0.00$	$52.8 \pm 0.56$	$53.1 \pm 0.30$
/m/01lb5	Chess	740	$0.7 \pm 0.00$	$51.9 \pm 0.70$	$50.9 \pm 1.23$
/m/03jqf3	Chevrolet silverado	115	$4.3 \pm 0.00$	$54.1 \pm 2.64$	$54.6 \pm 2.78$
/m/058qzx	Kitchen knife	360	$1.5 \pm 0.15$	$50.9 \pm 0.64$	$53.9 \pm 0.44$
/m/0cl6l	Straw	547	$1.0 \pm 0.10$	$50.3 \pm 0.33$	$51.0 \pm 0.55$
/m/0dlgzb	Bakmi	191	$2.6 \pm 0.00$	$51.8 \pm 0.83$	$51.2 \pm 0.68$
/m/0322v8	Lugger	103	$4.9 \pm 0.00$	$53.8 \pm 1.62$	$53.8 \pm 1.47$
/m/0dvg9	Ancient roman architecture	589	$0.8 \pm 0.00$	$48.5 \pm 0.96$	$47.1 \pm 1.03$
/m/019mbd	Antenna	545	$1.0 \pm 0.08$	$47.4 \pm 0.21$	$48.0 \pm 0.65$
/m/0b97cn	Lamian	257	$1.9 \pm 0.00$	$47.8 \pm 1.11$	$48.2 \pm 0.64$
/m/03lnzv	Calabaza	870	$0.6 \pm 0.05$	$46.0 \pm 0.35$	$45.8 \pm 0.34$
/m/09l0j_	Ring	676	$0.7 \pm 0.00$	$45.2 \pm 0.47$	$45.4 \pm 0.39$
/m/01y2w	Ciconiiformes	426	$1.2 \pm 0.10$	$45.2 \pm 0.82$	$45.2 \pm 0.49$
/m/02zkn_	Log cabin	448	$1.1 \pm 0.00$	$44.9 \pm 1.20$	$45.7 \pm 0.46$
/m/01l4_3	Bowed string instrument	728	$0.7 \pm 0.06$	$44.4 \pm 0.32$	$44.7 \pm 0.42$
/m/05z55	Pasta	954	$0.5 \pm 0.00$	$43.7 \pm 0.34$	$43.8 \pm 0.51$
/m/047fr	Knitting	409	$1.3 \pm 0.11$	$43.5 \pm 0.72$	$42.8 \pm 1.09$
/m/01xc8d	Rope	618	$0.8 \pm 0.00$	$43.0 \pm 0.39$	$42.8 \pm 0.25$

Table 7: **Middle  $\frac{1}{3}$  of classes from Openimages for active search.** (2 of 3) Recall (%) of positives for each selected class (153 total) from OpenImages with a labeling budget of 2,000 examples. Classes are in descending order based on the performance gain of MLP-SEALS over Random-All.

Label Name	Display Name	Total Positives	Random (All)	MLP (SEALS)	MLP (All)
/m/02n7rn	Paddy field	468	$1.1 \pm 0.10$	$42.6 \pm 0.57$	$44.2 \pm 1.05$
/m/05h35z	Formula racing	351	$1.4 \pm 0.00$	$42.6 \pm 0.74$	$41.4 \pm 0.37$
/m/02mk9	Engine	656	$0.8 \pm 0.00$	$41.7 \pm 0.46$	$40.6 \pm 1.81$
/m/0111f78	Shrimp	907	$0.6 \pm 0.00$	$40.4 \pm 0.55$	$40.8 \pm 0.48$
/m/01s0ps	Electric piano	345	$1.5 \pm 0.13$	$40.9 \pm 1.73$	$42.1 \pm 0.78$
/m/03fwl	Goat	1190	$0.4 \pm 0.00$	$39.6 \pm 0.57$	$39.6 \pm 0.23$
/m/0642b4	Cupboard	898	$0.6 \pm 0.06$	$39.6 \pm 0.46$	$39.6 \pm 0.34$
/m/0gv1x	Parrot	1546	$0.4 \pm 0.08$	$39.2 \pm 0.30$	$38.8 \pm 0.28$
/m/0dqb5	Citrus	796	$0.7 \pm 0.11$	$39.3 \pm 0.61$	$39.6 \pm 0.09$
/m/0cfk35	Chocolate truffle	288	$1.8 \pm 0.16$	$39.6 \pm 2.56$	$39.9 \pm 2.19$
/m/0dxb5	Berry	874	$0.6 \pm 0.05$	$37.8 \pm 0.47$	$37.6 \pm 0.30$
/m/0111r	Briefs	539	$1.0 \pm 0.08$	$37.1 \pm 0.36$	$37.2 \pm 0.57$
/m/01_6hg	Delicatessen	196	$2.6 \pm 0.00$	$38.2 \pm 0.76$	$39.0 \pm 0.46$
/m/0dwxr	Modern pentathlon	772	$0.6 \pm 0.00$	$35.9 \pm 5.45$	$32.6 \pm 12.85$
/m/0335ws	Concert dance	357	$1.4 \pm 0.00$	$36.6 \pm 0.67$	$36.1 \pm 0.69$
/m/0c0ygc	Stallion	598	$0.9 \pm 0.09$	$35.7 \pm 0.56$	$36.3 \pm 0.70$
/m/0176mf	Belt	467	$1.1 \pm 0.00$	$35.2 \pm 0.35$	$34.9 \pm 0.48$
/m/01czv3	Fortification	287	$1.7 \pm 0.00$	$35.7 \pm 1.75$	$37.6 \pm 0.90$
/m/01295w	Galliformes	674	$0.7 \pm 0.00$	$33.9 \pm 0.67$	$33.9 \pm 0.62$
/m/03931h	Stele	450	$1.1 \pm 0.00$	$33.9 \pm 0.96$	$32.7 \pm 1.46$
/m/03vd46	Herd	648	$0.8 \pm 0.07$	$33.5 \pm 0.44$	$33.7 \pm 0.35$
/m/0hlw	Algae	426	$1.2 \pm 0.00$	$33.8 \pm 1.30$	$33.1 \pm 1.24$
/m/0h8n982	Shelving	810	$0.7 \pm 0.15$	$33.2 \pm 0.31$	$33.3 \pm 0.11$
/m/01d7ng	Pelecaniformes	457	$1.1 \pm 0.10$	$33.4 \pm 9.74$	$37.5 \pm 0.40$
/m/02hnl	Drums	741	$0.7 \pm 0.00$	$32.9 \pm 0.40$	$32.7 \pm 0.25$
/m/04fyb1	Sirloin steak	297	$1.8 \pm 0.15$	$33.9 \pm 0.99$	$32.7 \pm 1.13$
/m/025_v	Cactus	377	$1.3 \pm 0.00$	$33.4 \pm 1.57$	$35.2 \pm 1.33$
/m/020dp	Cranberry	450	$1.2 \pm 0.10$	$32.9 \pm 0.83$	$33.7 \pm 0.81$
/m/0168g6	Factory	333	$1.5 \pm 0.00$	$32.0 \pm 0.81$	$31.7 \pm 1.25$
/m/04s5jq	Costume design	818	$0.6 \pm 0.00$	$30.9 \pm 1.45$	$30.6 \pm 1.17$
/m/05mfbz	Optical instrument	649	$0.8 \pm 0.00$	$30.3 \pm 5.72$	$32.8 \pm 0.52$
/m/01jnzj	Construction	515	$1.0 \pm 0.00$	$30.1 \pm 0.90$	$31.1 \pm 0.57$
/m/01cv4r	Temperate coniferous forest	328	$1.5 \pm 0.00$	$30.1 \pm 0.77$	$27.6 \pm 2.75$
/m/033cnk	Egg (Food)	1193	$0.4 \pm 0.00$	$28.8 \pm 3.17$	$28.6 \pm 3.04$
/m/0wgq98_	Skating	561	$1.0 \pm 0.16$	$28.8 \pm 5.85$	$30.4 \pm 1.88$
/m/02pkr5	Plumbing fixture	2124	$0.3 \pm 0.05$	$27.9 \pm 0.48$	$27.9 \pm 0.28$
/m/0g9vs81	Steamed rice	580	$0.9 \pm 0.00$	$28.1 \pm 1.48$	$30.2 \pm 1.37$
/m/0cyz6w	Whole food	708	$0.7 \pm 0.00$	$27.7 \pm 0.86$	$27.5 \pm 0.44$
/m/09qkx	Boardsport	673	$0.8 \pm 0.07$	$26.8 \pm 0.20$	$26.5 \pm 0.66$
/m/0frq6	Pork	464	$1.1 \pm 0.00$	$26.3 \pm 1.03$	$26.6 \pm 1.65$
/m/01w5c_	Aerial photography	931	$0.6 \pm 0.06$	$25.8 \pm 0.26$	$26.1 \pm 0.40$
/m/01wkk9	Town square	617	$0.8 \pm 0.00$	$25.7 \pm 0.90$	$26.1 \pm 0.82$
/m/0cffdh	Maple	2301	$0.2 \pm 0.02$	$24.3 \pm 0.53$	$24.4 \pm 0.50$
/m/038t8_	Estate	667	$0.9 \pm 0.13$	$24.8 \pm 1.22$	$25.9 \pm 0.54$
/m/01xq0k1	Cattle	5995	$0.1 \pm 0.01$	$23.8 \pm 0.13$	$23.6 \pm 0.32$
/m/0btmb	Superhero	968	$0.6 \pm 0.06$	$23.4 \pm 3.08$	$23.3 \pm 1.42$
/m/011lx7	Bracelet	770	$0.6 \pm 0.00$	$23.2 \pm 5.38$	$24.8 \pm 0.29$
/m/033kf	Frost	483	$1.0 \pm 0.00$	$23.1 \pm 1.93$	$22.5 \pm 2.67$
/m/01rh7y	Scale model	667	$0.8 \pm 0.13$	$22.9 \pm 1.02$	$23.7 \pm 4.30$
/m/0f6x8	Bird of prey	712	$0.7 \pm 0.00$	$22.4 \pm 0.66$	$22.0 \pm 0.51$
/m/01pvk	Canal	726	$0.7 \pm 0.06$	$22.4 \pm 0.46$	$20.9 \pm 1.09$

Table 8: **Bottom  $\frac{1}{3}$  of classes from Openimages for active search.** (3 of 3) Recall (%) of positives for each selected class (153 total) from OpenImages with a labeling budget of 2,000 examples. Classes are in descending order based on the performance gain of MLP-SEALS over Random-All.

Label Name	Display Name	Total Positives	Random (All)	MLP (SEALS)	MLP (All)
/m/02mwzg	Plateau	452	$1.1 \pm 0.00$	$22.7 \pm 0.50$	$19.1 \pm 3.54$
/m/01n5cy	Carpet	644	$0.8 \pm 0.07$	$21.9 \pm 5.41$	$22.7 \pm 0.95$
/m/0j_5b	Monoplane	756	$0.7 \pm 0.07$	$21.8 \pm 2.08$	$20.1 \pm 1.43$
/m/0fq22vb	Exhibition	513	$1.0 \pm 0.09$	$21.9 \pm 0.45$	$23.1 \pm 0.38$
/m/03vtj	Ice	682	$0.8 \pm 0.07$	$21.6 \pm 1.04$	$23.1 \pm 3.43$
/m/0cnmr	Fur	834	$0.6 \pm 0.07$	$21.2 \pm 0.97$	$17.3 \pm 9.06$
/m/02qm2x	Icing	1118	$0.4 \pm 0.00$	$20.5 \pm 0.59$	$20.1 \pm 0.26$
/m/01c34b	Flooring	814	$0.6 \pm 0.05$	$20.4 \pm 0.46$	$16.9 \pm 8.97$
/m/0hkvx	Prairie	792	$0.6 \pm 0.00$	$19.0 \pm 1.00$	$19.2 \pm 0.50$
/m/0cnxs6x	Tooth	976	$0.5 \pm 0.05$	$18.6 \pm 2.01$	$18.0 \pm 2.36$
/m/0bpn3c2	Skateboarding Equipment	862	$0.6 \pm 0.05$	$18.1 \pm 6.15$	$19.3 \pm 4.83$
/m/0h8ls87	Automotive exterior	1060	$0.5 \pm 0.04$	$17.7 \pm 2.93$	$11.9 \pm 10.03$
/m/03tqj	Icon	186	$2.7 \pm 0.00$	$19.9 \pm 0.85$	$17.2 \pm 4.82$
/m/0gd2v	Marine mammal	2954	$0.2 \pm 0.03$	$17.3 \pm 0.45$	$17.2 \pm 0.46$
/m/03nxtz	Cottage	670	$0.7 \pm 0.00$	$17.6 \pm 0.57$	$17.3 \pm 0.47$
/m/099md	Soldier	1032	$0.5 \pm 0.09$	$17.3 \pm 0.69$	$16.8 \pm 0.64$
/m/07k1x	Tool	1549	$0.3 \pm 0.03$	$17.0 \pm 0.64$	$16.9 \pm 0.65$
/m/02zfvv	American shorthair	2084	$0.3 \pm 0.03$	$16.5 \pm 0.42$	$16.7 \pm 0.59$
/m/0541p	Multimedia	741	$0.7 \pm 0.06$	$16.8 \pm 2.04$	$17.1 \pm 0.99$
/m/0hr8	Asphalt	1026	$0.5 \pm 0.04$	$15.1 \pm 0.71$	$11.5 \pm 5.95$
/m/09l65	Singer	604	$0.9 \pm 0.07$	$14.6 \pm 7.10$	$13.6 \pm 7.03$
/m/0j6jq	Floodplain	567	$0.9 \pm 0.00$	$14.6 \pm 1.33$	$14.0 \pm 1.40$
/m/01f4td	Rural area	921	$0.6 \pm 0.05$	$14.2 \pm 0.36$	$13.2 \pm 0.91$
/m/03hcy1d	Mitsubishi	511	$1.0 \pm 0.09$	$12.6 \pm 0.30$	$11.8 \pm 1.11$
/m/013y0j	Organ (Biology)	1156	$0.5 \pm 0.12$	$12.1 \pm 8.09$	$15.9 \pm 5.12$
/m/0641k	Paper	969	$0.5 \pm 0.00$	$12.0 \pm 6.63$	$14.8 \pm 1.73$
/m/0jqb	Annual plant	677	$0.7 \pm 0.00$	$11.8 \pm 1.16$	$10.7 \pm 2.90$
/m/02vwbzz	Electric blue	1180	$0.5 \pm 0.05$	$11.5 \pm 1.07$	$9.4 \pm 4.96$
/m/019cfy	Stadium	1654	$0.3 \pm 0.03$	$10.8 \pm 0.83$	$9.3 \pm 2.35$
/m/04rd7	Mural	649	$0.8 \pm 0.14$	$10.4 \pm 2.13$	$10.3 \pm 1.19$
/m/03jvv0	Teal	975	$0.5 \pm 0.05$	$9.9 \pm 0.46$	$10.4 \pm 0.27$
/m/09qqq	Wall	1218	$0.4 \pm 0.04$	$9.3 \pm 8.06$	$12.0 \pm 6.49$
/m/01bmhj	Thumb	895	$0.6 \pm 0.06$	$9.3 \pm 7.45$	$13.8 \pm 2.69$
/m/01jfm_	Vehicle registration plate	5697	$0.1 \pm 0.01$	$8.7 \pm 0.99$	$8.3 \pm 2.07$
/m/025sv9y	Landscaping	789	$0.7 \pm 0.06$	$9.2 \pm 2.03$	$9.3 \pm 1.41$
/m/03s7w_	Cirque	347	$1.5 \pm 0.13$	$9.9 \pm 2.53$	$9.8 \pm 1.88$
/m/0krfg	Meal	1250	$0.4 \pm 0.07$	$8.5 \pm 2.97$	$9.1 \pm 2.57$
/m/023bbt	Wilderness	1225	$0.4 \pm 0.00$	$8.5 \pm 4.58$	$9.8 \pm 2.46$
/m/06wqb	Space	1006	$0.5 \pm 0.04$	$7.8 \pm 5.14$	$6.3 \pm 5.74$
/m/04qgp	Liqueur	539	$1.0 \pm 0.17$	$8.0 \pm 6.36$	$12.8 \pm 4.37$
/m/09q2t	Brown	1427	$0.4 \pm 0.03$	$7.2 \pm 5.31$	$2.6 \pm 4.79$
/m/01sgl	Cycling	794	$0.6 \pm 0.00$	$7.3 \pm 2.08$	$7.8 \pm 2.42$
/m/05nnm	Organism	1148	$0.4 \pm 0.00$	$6.8 \pm 3.70$	$2.0 \pm 2.82$
/m/01j3sz	Laugh	750	$0.7 \pm 0.06$	$6.6 \pm 2.98$	$8.6 \pm 1.07$
/m/01dv4h	Portrait	2510	$0.2 \pm 0.02$	$5.8 \pm 0.98$	$5.3 \pm 0.70$
/m/02mnkq	Bumper	985	$0.5 \pm 0.06$	$5.9 \pm 4.01$	$8.3 \pm 3.49$
/m/079bkr	Mode of transport	1387	$0.4 \pm 0.04$	$5.1 \pm 2.18$	$3.6 \pm 2.87$
/m/01ckgp	Interaction	924	$0.6 \pm 0.12$	$4.5 \pm 3.72$	$4.6 \pm 2.64$
/m/012sbd	Tournament	841	$0.6 \pm 0.07$	$4.3 \pm 2.23$	$5.1 \pm 1.23$
/m/05qjc	Performing arts	1030	$0.5 \pm 0.00$	$2.3 \pm 0.89$	$2.5 \pm 0.77$
/m/083jv	White	1494	$0.3 \pm 0.00$	$2.0 \pm 1.19$	$0.5 \pm 0.16$